

# Plasma-driven solution electrolysis F


Cite as: J. Appl. Phys. **129**, 200902 (2021); <https://doi.org/10.1063/5.0044261>

Submitted: 15 January 2021 • Accepted: 05 March 2021 • Published Online: 24 May 2021

 Peter J. Bruggeman,  Renee R. Frontiera,  Uwe R. Kortshagen, et al.

## COLLECTIONS

Paper published as part of the special topic on [Plasma-Liquid Interactions](#)

 This paper was selected as Featured



View Online



Export Citation



CrossMark

## ARTICLES YOU MAY BE INTERESTED IN

[The essential role of the plasma sheath in plasma-liquid interaction and its applications—A perspective](#)

Journal of Applied Physics **129**, 220901 (2021); <https://doi.org/10.1063/5.0044905>

[Plasma-liquid interactions](#)

Journal of Applied Physics **130**, 200401 (2021); <https://doi.org/10.1063/5.0078076>

[Plasma physics of liquids—A focused review](#)

Applied Physics Reviews **5**, 031103 (2018); <https://doi.org/10.1063/1.5020511>

Lock-in Amplifiers  
up to 600 MHz



Zurich  
Instruments

















# Plasma-driven solution electrolysis

Cite as: J. Appl. Phys. **129**, 200902 (2021); doi: [10.1063/5.0044261](https://doi.org/10.1063/5.0044261)

Submitted: 15 January 2021 · Accepted: 5 March 2021 ·

Published Online: 24 May 2021



Peter J. Bruggeman,<sup>1,a)</sup>  Renee R. Frontiera,<sup>2</sup>  Uwe R. Kortshagen,<sup>1</sup>  Mark J. Kushner,<sup>3</sup>  Suljo Linic,<sup>4</sup>   
George C. Schatz,<sup>5</sup>  Himashi Andaraarachchi,<sup>1</sup>  Stephen Exarhos,<sup>1</sup>  Leighton O. Jones,<sup>5</sup>   
Chelsea M. Mueller,<sup>5</sup>  Christopher C. Rich,<sup>2</sup>  Chi Xu,<sup>1</sup>  Yuanfu Yue,<sup>1</sup>  and Yi Zhang<sup>4</sup> 

## AFFILIATIONS

<sup>1</sup>Department of Mechanical Engineering, University of Minnesota, 111 Church Street SE, Minneapolis, Minnesota 55455, USA

<sup>2</sup>Department of Chemistry, University of Minnesota, Minneapolis, Minnesota 55455, USA

<sup>3</sup>Department of Electrical Engineering and Computer Science, University of Michigan, 1301 Beal Ave., Ann Arbor, Michigan 48109-2122, USA

<sup>4</sup>Department of Chemical Engineering, University of Michigan, Ann Arbor, Michigan 48109, USA

<sup>5</sup>Department of Chemistry, Northwestern University, 2145 Sheridan Road, Evanston, Illinois 60208, USA

**Note:** This paper is part of the Special Topic on Plasma-Liquid Interactions.

**a)** Author to whom correspondence should be addressed: [pbruggem@umn.edu](mailto:pbruggem@umn.edu)

## ABSTRACT

Plasmas interacting with liquids enable the generation of a highly reactive interfacial liquid layer due to a variety of processes driven by plasma-produced electrons, ions, photons, and radicals. These processes show promise to enable selective, efficient, and green chemical transformations and new material synthesis approaches. While many differences are to be expected between conventional electrolysis and plasma-liquid interactions, plasma-liquid interactions can be viewed, to a first approximation, as replacing a metal electrode in an electrolytic cell with a gas phase plasma. For this reason, we refer to this method as plasma-driven solution electrochemistry (PDSE). In this Perspective, we address two fundamental questions that should be answered to enable researchers to make transformational advances in PDSE: *How far from equilibrium can plasma-induced solution processes be driven?* and *What are the fundamental differences between PDSE and other more traditional electrochemical processes?* Different aspects of both questions are discussed in five sub-questions for which we review the current state-of-the-art and we provide a motivation and research vision.

Published under license by AIP Publishing. <https://doi.org/10.1063/5.0044261>

## I. INTRODUCTION

Plasma-liquid interactions are an increasingly important focus area in the field of plasma science and technology.<sup>1</sup> Plasmas interacting with liquids yield a highly reactive interfacial liquid layer due to a variety of processes driven by plasma-produced electrons, ions, photons, and radicals. In this system, electrons are produced in a gas phase plasma and transport into the interfacing liquid, sometimes being injected into the interface by electric fields. This interfacial layer has drawn comparisons to conventional electrochemical systems, in which a solid electrode would directly generate solvated electrons in an electrolyte solution.<sup>1-4</sup> In contrast to conventional electrolysis, however, the high-power density in plasmas enables exceptionally large fluxes of electrons, some having high energies up to 10 eV or more with proper biasing, which lead to a high concentration of (solvated) electrons

in a near plasma-liquid interfacial region with a thickness up to a few tens of nm.<sup>5,6</sup> These conditions enable unique chemical transformations that may be unattainable by conventional electrolysis. While many differences between electrolysis and plasma-liquid interactions are to be expected—as discussed in this Perspective—plasma-liquid interactions can, to a first approximation, be viewed as replacing a metal electrode in an electrolytic cell with a gas phase plasma. This is a form of “electrodeless” electrochemistry. In this context, we will specifically refer to the plasma-induced liquid phase chemical transformations as plasma-driven solution electrochemistry (PDSE).

The past decade has seen rapid advances in our understanding of plasma-liquid interactions.<sup>1,7</sup> Applications such as contaminated water treatment, chemical conversion, and materials synthesis have motivated significant research efforts and expanded the field.<sup>8,9</sup>

Recently, plasma-produced electrons have been proposed as a key enabler for highly effective decomposition of perfluorooctanoic acid, an emerging water pollutant, with energy efficiencies exceeding conventional electrochemical and sonolytic processes.<sup>10</sup> Plasma was also shown to be an effective enabler of preparative organic chemistry, as demonstrated for electron-catalyzed trifluorination reactions by Gorbanev *et al.*<sup>11</sup> Plasma–liquid interactions have also enabled the synthesis of NH<sub>3</sub> with a Faradaic efficiency approaching 100%, although the energy cost was over 200 times larger than for the Haber–Bosch process due to the high energy required to generate electrons in a gas phase plasma (ionization energy of N<sub>2</sub> is 15.6 eV) and additional collisional and excitation energy losses in the plasma.<sup>12</sup> This experiment demonstrates both the potential of PDSE for the effective reduction of highly stable species such as N<sub>2</sub> requiring *multi-electron reduction processes* and the need for analogous figures of merit that extend beyond Faradaic electrochemistry models in PDSE.

PDSE also shows promise for the synthesis of high value-added materials such as nanoparticles. For example, plasma-driven reduction of Au<sup>3+</sup> enables the rapid synthesis of Au nanoparticles.<sup>13</sup> Maguire *et al.* compared the rate of nanoparticle synthesis in a solution using radiolysis and electron beam excitation.<sup>13</sup> The electron dose rate for the particular plasma source used in this experiment is moderate compared to electron beams, while the Au<sup>3+</sup> reduction rate per unit time and volume is two orders of magnitude larger. This large reduction rate was, in part, due to differences in the volume being treated and by the large electron flux to the liquid at much lower energies (1–10 eV) than is typical for electron beams (~keV–MeV). A 15 kW electron beam operating at 10 MeV has a current of 1.5 mA. An atmospheric pressure plasma has a higher power density and can for similar operating powers easily achieve a current that is three orders of magnitude larger. Thus, PDSE can achieve *high reaction yields* with the potential of possible *more selective chemistry* by lower electron energies.

Another example of “electrodeless” electrochemical material synthesis is the assembly of nanomaterials at the liquid–liquid interface between two immiscible electrolyte solutions.<sup>14</sup> This interface is similar to a metal–electrode/electrolyte solution interface and enables charge transfer and reduction/oxidation processes to occur at the interface. The liquid–liquid interface is a highly reproducible, defect-free surface that enables the controlled and selective assembly of a large variety of solid particles. While highly controlled reactions are enabled by this approach, the current density is typically only 10–100  $\mu\text{A cm}^{-2}$ .<sup>14,15</sup> The plasma–liquid interface is structurally similar. However, due to the high conductivity of the plasma, the plasma–liquid interface can sustain four orders of magnitude higher current densities. In addition, the plasma–liquid system provides the possibility of controlling electron fluxes on nanosecond time scales commensurate with the typical lifetimes of some reactive intermediates in solution. The analogy between liquid/liquid interfaces and plasma–liquid interfaces indicates that PDSE may be controlled to drive similarly selective chemistry but at higher rates.

Experiments dealing with the interaction of plasmas and liquids in the context of electrochemistry date back more than 100 years ago.<sup>16</sup> Most applications of PDSE explored to date have not

relied on selective reactions and chemical transformations. Controlling electron-driven chemistry requires an in-depth understanding of the energetics and transport of solution phase species including electrons and ions. This need for understanding particularly includes the exotic properties of the near interfacial liquid layer, which contains high concentrations of short-lived reactive species and is likely to be critical to obtaining the potential benefits of PDSE.<sup>1</sup> Gaining a fundamental insight into these processes may lead to transformational advances in new materials synthesis and in our ability to use plasmas for selective, efficient, and green chemical transformation.

The current fundamental understanding of plasma–liquid interactions and PDSE have been summarized in detail in a recent roadmap<sup>1</sup> and more extended in reviews.<sup>3,7,17</sup> In this Perspective, we propose and discuss a set of key science questions that we believe should be answered to drive transformational advances in PDSE.

## II. SCIENTIFIC QUESTIONS

In gas phase plasmas, it is possible to have rapidly rising voltage pulses that yield electric fields that greatly exceed those in the steady state. The resulting high electric fields push the plasma into a state of non-equilibrium, generating species that are not produced in steady-state equilibrium conditions, which in turn enable synthesis of, for example, unique nanomaterials. Non-equilibrium in plasmas most often refers to the different kinetic energies between electrons, neutral, and ionic species. Important aspects of non-equilibrium also include production of electronically and vibrationally excited species and, in extension, any energetic species in excess of what is present under equilibrium conditions. This excess of specific species produces unique phenomena and chemistry. A well-known example is O<sub>3</sub> generation in dielectric barrier discharge (DBD) plasmas from O<sub>2</sub>, which exploits the highly non-equilibrium properties (high electron energies for gas temperatures near room temperature) of DBD plasmas at atmospheric pressure. High electron energies enable the dissociation of oxygen, the highly collisional environment enables three-body recombination of O with O<sub>2</sub> forming O<sub>3</sub>, and the low gas temperature suppresses thermal dissociation of O<sub>3</sub>.<sup>18</sup>

While non-equilibrium processes in a gas phase plasma are readily achieved, PDSE occurs at or near the interface of a non-equilibrium gas phase plasma and a solution. It is unclear how and if gas phase non-equilibrium properties are transferred into the solution phase. This motivates our first overarching scientific question: *How far from equilibrium can plasma-driven solution processes be driven?*

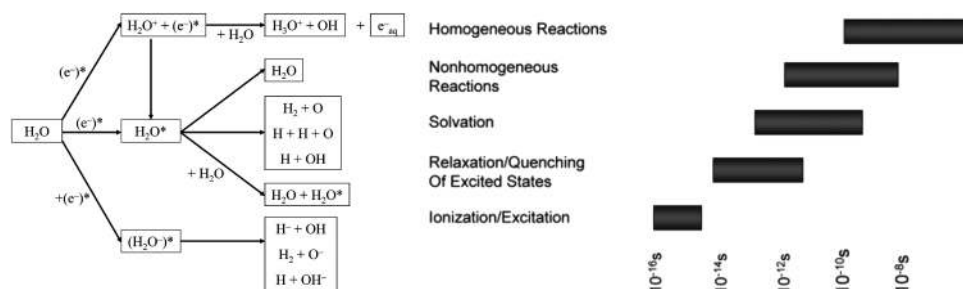
Restoring equilibrium depends on collision frequency, which in liquids is orders of magnitude larger than in the gas phase. Therefore, it is more challenging to achieve non-equilibrium in the liquid phase. That said, the injection of highly reactive species from the plasma does lead to non-equilibrium compositions at the plasma–liquid interface for some finite time and distance. The large concentrations of reactive species have much larger spatial gradients than in the gas phase due to their relatively slow diffusive transport in solution, and these large gradients can enable localized non-equilibrium conditions. We explore the non-equilibrium aspects of PDSE in this Perspective focusing on

electrons, ions, electric fields, charging, photons, and kinetically driven processes by means of the following five sub-questions:

- To what extent do hot electrons play a role in PDSE?
- Do ion-induced sputtering and energy released by ion recombination and neutralization impact PDSE?
- How do strong electric fields, interfacial charging, and double layers at the plasma–liquid interface impact PDSE?
- How does plasma impact the solvation structure and dynamics near the plasma–liquid interface?
- Can the large fluxes and correspondingly large densities of reactive species at the plasma–liquid interface lead to liquid phase processes away from equilibrium driven by chemical kinetics?

While PDSE has been successfully utilized in a multitude of applications, the list of proposed processes introduced by plasma–liquid interactions that enable or impact these applications is long. The uniqueness of the plasma-driven process is an important issue as there is overlap with several processes that underpin traditional electrochemistry. The anticipated advantages of PDSE include its potential for high yields and sustainable green technology enabling selective multi-electron reduction processes. However, it is unclear how mechanistic differences between PDSE and conventional electrochemistry and possible non-equilibrium effects in PDSE may influence proposed applications or outcomes. This leads us to the second overarching science question: *What are the fundamental differences between PDSE and other more traditional electrochemical processes?* Different aspects of this question will be discussed by means of the following five sub-questions that address different aspects of PDSE while contrasting plasma-driven processes with more traditional electrochemical processes:

- What is the relative importance of electron, ion, radical, and photon-induced processes in PDSE and to what extent can each be separately controlled?
- What is the PDSE equivalent of manipulating the electrode potential in conventional electrochemistry to enable selective redox processes?
- What are the key differences in transport limited chemical conversion in electrochemistry and PDSE?
- Are current models capable of quantitatively describing the fundamental PDSE processes?
- What are optimal methods to quantify the fundamental PDSE processes experimentally?



In the remainder of this article, we address the above questions by describing the motivation behind the question, reviewing the state-of-the-art in this area, and formulating our perspective.

### III. HOW FAR FROM EQUILIBRIUM CAN PLASMA-INDUCED SOLUTION PROCESSES BE DRIVEN?

#### A. To what extent do hot electrons play a role in PDSE?

##### 1. Motivation

At the plasma–liquid interface in PDSE, the anode-plasma sheath can transport electrons from the gas phase to the liquid phase. Electrons in this process are essentially free and can induce different reaction pathways, including direct reduction and indirect reduction following solvation. In analogy with gas phase collisions, if the incident electron energy is more than 4 eV, it can lead to electronic excitation of water and possibly electron-induced impact dissociation or ionization of water at higher electron energies.<sup>19</sup> Lower energy electrons can produce vibrational excitation and heating of the water molecules at the surface, possibly accelerating endothermic reactions. The intensity of the electron flux and the electron energy distribution are expected to strongly influence any electron-induced reactions in PDSE.

##### 2. State-of-the-art

Studies on the radiolysis of water have established a detailed understanding of electron-induced reactions in water and their products.<sup>20</sup> An overview of reactions induced by ionizing radiation in water and the corresponding relevant reaction time scales are shown in Fig. 1.<sup>21</sup> There is growing evidence that reduction can occur on time scales shorter than the electron solvation time scale, which is in the 0.3–1.0 ps range.<sup>22</sup> For example, pulsed radiolysis studies suggest (but do not directly measure) that water ionization by hot electrons, followed by hydration of the resulting water ion,  $\text{H}_2\text{O}^+ + \text{H}_2\text{O} \rightarrow \text{OH} + \text{H}_3\text{O}^+$ , occurs on a time scale of a few tens of femtoseconds. Electron recombination with  $\text{H}_3\text{O}^+$  can also occur in <100 fs,<sup>23</sup> however, these times depend on the total density of the reactants as recombination scales with the square of the charge density. Very short time scales for  $e^- + \text{H}_3\text{O}^+$  have also been noted in ultrafast UV photolysis studies,<sup>24</sup> but isotope studies indicate that after the electron is solvated, recombination with  $\text{H}_3\text{O}^+$  is much slower, on the order of hundreds of picoseconds. Presumably, more rapid recombination of the solvated electron is inhibited by its

**FIG. 1.** Reactions induced by ionizing radiation in water and their relevant time scales. The initial reactions include electron-induced ionization and excitation of water and electron attachment to water. Reprinted with permission from Garrett *et al.*, Chem. Rev. **105**, 355–390 (2005). Copyright 2005 American Chemical Society.

surrounding water molecules. In another study, pulse radiolysis leading to the reduction of  $\text{Ag}^+$  in aqueous solutions was measured to be ultrafast (less than a few 100 fs). However, solvated electrons recombine with  $\text{Ag}^+$  on much longer diffusion-limited time scales with a reaction rate of  $4 \times 10^{10} \text{ M}^{-1} \text{ s}^{-1}$ .<sup>25</sup> The current state-of-the-art knowledge on the reactivity of short-lived species in irradiated water at ultrafast (femtoseconds to picoseconds) time scales is thus limited. While the energies of electrons in radiolysis are in the keV–MeV range, substantially higher than the 1–10 eV range pertinent to PDSE, the high energy electrons in radiolysis thermalize in collisions in solution and ultimately will participate in similar reactions as in PDSE.

The ultrafast processes observed in photolysis and radiolysis through the use of pico- and femtosecond lasers have not been studied in plasmas due to challenges with initiating plasma interactions on ultrafast time scales. The state-of-the-art plasma–liquid interaction models are challenged by resolving electron solvation time scales. Gopalakrishnan *et al.* observed a significant increase in the electric field in the anode layer ( $\sim 50 \mu\text{m}$ ) near the liquid reaching 7 kV/cm in a particle-in-cell/Monte Carlo collision simulation of a DC glow discharge configuration with a liquid anode (Fig. 2).<sup>6</sup> The model suggests that most electrons impact the water surface with energies between 5 and 12 eV. Meesungnoen *et al.* reported results from a Monte Carlo simulation of electrons interacting with liquid water at 298 K showing penetration depths of  $\sim 10 \text{ nm}$  for electrons with an energy of about 10 eV.<sup>26</sup> Interestingly, the predicted penetration depth of solvated electrons assuming thermalization is of the same order of magnitude.<sup>6</sup> Recent photoelectron studies at larger

energies (70–900 eV) show that the mean free path of electrons in water is somewhat higher than in other materials, such as PMMA, and therefore above the “universal curve” estimate, which is also about 10 nm at 10 eV.<sup>27</sup> Non-thermalized electrons could, therefore, not only enhance reactivity at the plasma–liquid interface due to ultrafast chemical kinetics but could also impact the spatial distribution of solvated electrons near the interface. Reactor scale plasma–liquid water models typically do not resolve the penetration depth of electrons prior to solvating. In these models, incoming electrons from the plasma effectively transform to solvated electrons at the surface of the water. For computational expediency, these simulations may dial down the rate of solvation to lengthen integration time steps without significantly altering the outcome. The rate of solvation only needs to be much faster than any other process.<sup>28</sup>

### 3. Perspective

While high energy electron chemistry (keV–MeV) has been explored in radiolysis, electron energies typical for PDSE (1–10 eV) have received little attention in the context of driving chemical reactions in solutions. Such studies are challenged by the range of plasma-produced species, limited control over electron energy distributions, poorly understood structure and boundary conditions at the plasma–liquid interface, and a lack of ultrafast time-resolved studies including theory work.

## B. Do ion-induced sputtering and energy released by ion recombination and neutralization impact PDSE?

### 1. Motivation

Ion-induced sputtering and ion recombination and neutralization are processes where non-equilibrium effects could play an important role in PDSE. These processes can only be described quantitatively by molecular-level theory, and so they are included in current plasma–liquid models using rate coefficients analogous to gas phase processes.<sup>29</sup> Ion-induced processes can impact both the gas and liquid phase near the plasma–liquid interface and hence significantly impact PDSE.

### 2. State-of-the-art

It is common in plasma–liquid interface models to assume that the potential energy of all cations is large compared to any activation energy barrier required to enter the liquid. Indeed, ions will likely spend little time at the surface as we expect very rapid solvation (1 ps) followed by 10–100 ps of vibrational relaxation (Fig. 1).<sup>21</sup> The only exception is when the electron affinity of the ion is larger than the ionization energy of water, in which case there will be an electron transfer at the point of collision, followed by hydration and relaxation. Tochikubo *et al.* concluded that ion irradiation of electrolyte solutions leads to acidification consistent with the above charge transfer collisions between low-energy incident positive ions and water molecules, which leads to the generation of  $\text{H}_3\text{O}^+$ .<sup>30</sup> Delgado *et al.* proposed that direct ionization of water by, e.g.,  $\text{Ar}^+$  ions impinging on the liquid could lead to the formation of an  $e^-$  in the conduction band of liquid water that could act as a source for secondary electron emission from the liquid.<sup>31</sup>

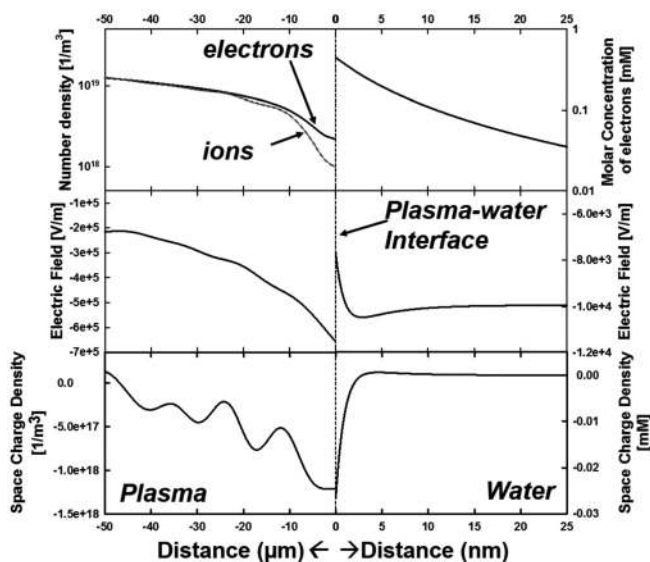


**FIG. 2.** Structure of the plasma–liquid interface in a DC glow discharge modeled by a particle-in-cell/Monte Carlo collision simulation. The liquid acts as an anode for the gas phase plasma and is a 100 mM NaCl solution. The figure shows the electron densities/concentrations, the electric field profiles, and the space charge both in the gas and liquid phase. Reproduced with permission from Gopalakrishnan *et al.*, *J. Phys. D: Appl. Phys.* **49**, 295205 (2016). Copyright 2016 IOP Publishing.



Ion-electron recombination thermodynamics involves a trade-off between two factors: (1) energy release associated with electron transfer that leads to neutralization and (2) the difference in the solvation energy of ions compared to the neutralized products. In some cases, the overall energy release can be surprisingly small—for example, the  $e^- + H^+$  recombination releases 13.6 eV in the gas phase—but after including solvation energies in liquids, the energy release is about 1 eV. Donald *et al.* reported measured free energy changes for several common transition metal complexes.<sup>32</sup> However, thermodynamic properties do not necessarily reflect kinetics.

Sputtering by ion bombardment can provide significant local energy release to the region around the liquid where the ion impacts,<sup>33</sup> as well as significant primary and secondary reactions.<sup>34</sup> The initial excitation could be translational or electronic. Minagawa *et al.* studied  $O^+$  ions in the range of 10–100 eV impacting liquid water and showed that localized liquid temperature can increase in excess of 1000 K at the penetration depth of the ion, which relaxes back to ambient temperatures within  $\sim 6$  ps (see Fig. 3).<sup>35</sup> Nikiforov studied  $O_2^+$  ion-impact sputtering on the liquid surface using a molecular dynamics simulation for ion energies between 50 and 500 eV.<sup>36</sup> The results showed that the sputtering yield of water molecules depends on the ion energy, ranging from 2 to 450 molecules/ion within this energy range. Most studies of ion-induced sputtering, as the ones described above, are performed with large ion energies, but such large ion energies may not be representative of processes induced by the lower ion energies striking surfaces of no more than a few eV in atmospheric pressure plasmas. However, simulations have shown that in the high sheath electric fields that occur when streamers strike a liquid surface, ions with energies as high as 35–45 eV can be produced.<sup>37</sup> There may also be differences as a function of ion energy that go beyond sputtering yield and penetration depth. For example, incident ions with an energy of 100 eV can reflect from a liquid surface due to a strong repulsive Coulombic force when H atoms of the water molecules at the surface are facing the impinging ion. In contrast, for 10 eV ion energies, it has been shown that even if the hydrogen atoms of the water molecules are facing an  $O^+$  ion, the water molecules rotate very rapidly within 0.03 ps to reduce the repulsive force.<sup>35</sup>

Sirotkin and Titov noted that the positive ion sputtering of a liquid cathode leads to transfer of both solvent and solute into the gas phase and that this process significantly modifies the cathode layer.<sup>38</sup> Specifically, metal cations with low ionization potential lead to a significant reduction of the cathode fall voltage. The transfer efficiency of metal cations to the gas phase was found to depend on the hydration energy of the cations. The energy deposition due to ion current into the liquid cathode might significantly enhance the energy transfer from the plasma, which could lead to systems where dominant reactive species fluxes are similar or smaller than water molecule fluxes toward the gas phase. This implies an important bi-directional transport at the gas–liquid interface.<sup>39,40</sup>

### 3. Perspective

Both ion recombination and sputtering provide examples of where very little is known about the fundamental processes at the molecular level from either theory or experiment, particularly for the

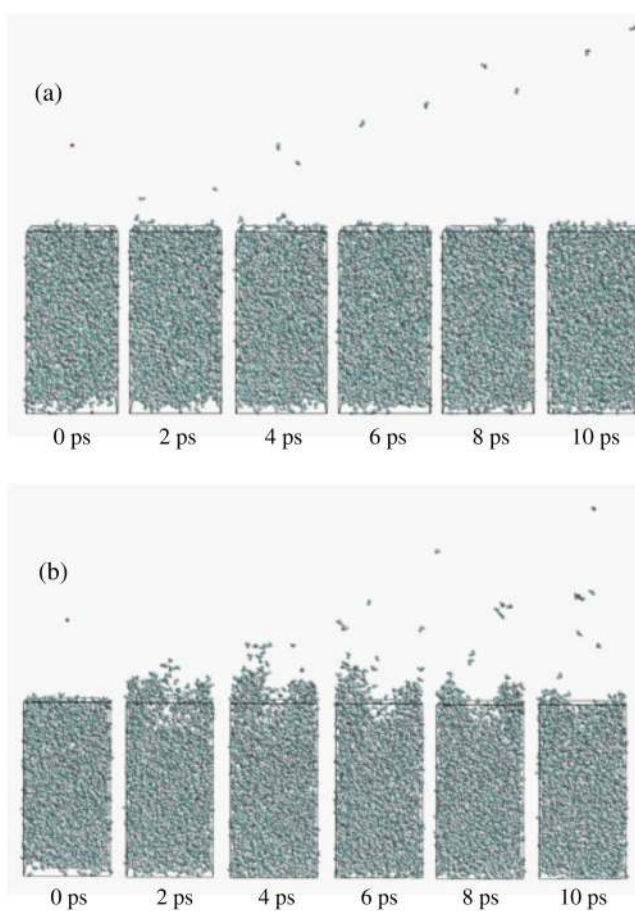


**FIG. 3.** Effect of  $O^+$  ion bombardment from an atmospheric pressure plasma to a liquid surface by classical molecular dynamics simulation. The number of sputtered water molecules, liquid temperature, and ion penetration depth in the liquid were investigated after  $O^+$  ions with kinetic energies of 10 eV (a) and 100 eV (b) impinging on the liquid surface. The average number of sputtered water molecules per ion is 0.5 and 7 for 10 and 100 eV, respectively. Reprinted with permission from Minagawa *et al.*, *Jpn. J. Appl. Phys.* **53**, 010210 (2013). Copyright 2013 The Japan Society of Applied Physics.

low ion energies relevant to PDSE. While numerical studies indicate a strong influence of the ion energy on interfacial kinetics, experimental investigations of these phenomena have been limited. It is necessary to investigate the impact of ion sputtering and ion-induced reactions with more controllable ion energies. Studies in low pressure plasmas with low vapor pressure liquids may be one route to achieve this goal.

## C. How do strong electric fields, interfacial charging, and double layers at the plasma–liquid interface impact PDSE?

### 1. Motivation

The presence of plasma-induced electric fields and/or charge deposition can induce a variety of physical and chemical changes

to a liquid surface, including the orientation of molecular species and the formation of electrical double layers (EDLs). We anticipate that the effects of electric fields at the plasma–liquid interface and related space charge induced gradients in the liquid should strongly impact PDSE, although this has yet to be proven.

## 2. State-of-the-art

It is well known that a gas–liquid interface can become unstable when subjected to an electric field with a direction perpendicular to the interface, a phenomenon called electrohydrodynamic instability. This instability can lead to Taylor cone formation.<sup>41</sup> Interestingly, the critical electric field for a gas–water interface is very similar to the breakdown field in air,  $\sim 30 \text{ kV cm}^{-1}$ .<sup>42,43</sup>

The stability of the plasma–liquid interface in a DC-driven glow discharge is polarity dependent. When the solution is the cathode, the cathode layer typically becomes filamentary. When the solution is the anode, the anode layer remains diffuse.<sup>44</sup> These phenomena have been explained by the relatively large electric fields in the cathode sheath due to the small secondary electron emission coefficients for solutions. These high electric fields are in excess of the electrohydrodynamic instability limit of a gas–liquid water interface, where liquid interfacial deformation leads to local increases in the electric field and filament formation.<sup>1</sup> These instabilities can even lead to droplet ejection. The analytical chemistry literature cites this ejection as the reason trace ions can be present in large amounts in the gas phase and can be effectively used to analyze liquids by glow discharge emission spectroscopy.<sup>45</sup> Holgate *et al.* conducted linear perturbation analysis of the plasma–liquid interface for molten metals in the context of fusion plasmas and have shown that a positive ion flux can stabilize electrohydrodynamic instabilities for conductive liquids.<sup>46</sup> For glow discharges interacting with a solution anode, the discharge remains diffuse under nominal conditions. At higher currents, though, self-organization can occur at the surface resulting in symmetric patterns ranging from circular to star-like shapes, as observed from the emission of the plasma. This implies that the electric field is well below the electrohydrodynamic instability limit in this configuration.

While many models have addressed plasma–liquid interactions, only few models consider details of the interface and the space charge fields. The Debye length in solutions can have nanometer length scales and can be significantly smaller than the Debye length scale of most diffuse plasmas in contact with liquids ( $\sim 1 \mu\text{m}$ ). As a result, fluid models often do not resolve the length scales relevant for space charge formation in the liquid. Rumbach *et al.* have developed a simplified analytical model for the Debye layer formed at the plasma–liquid interface.<sup>47</sup> This model, while having simplifying assumptions, is capable of reproducing the experimental relation between plasma current density and the solution ionic strength (or conductivity). Still, some of the assumptions, such as a matrix electron sheath (ion density is zero in the sheath), are different than the results reported by Gopalakrishnan *et al.* (see also Fig. 2), which were obtained with a more detailed model.<sup>6</sup>

The above description is focused on steady-state sheaths. Transient plasma phenomena, however, are becoming exceedingly common in experiments because they tend to lead to more diffuse plasmas and hence homogeneous interactions with liquids on nanosecond up to microsecond time scales.<sup>48</sup> These times are

shorter than the typical time scales required for the development of electrohydrodynamic instabilities and Taylor cones. Typical solution conductivities range between  $5 \mu\text{S cm}^{-1}$  and  $1 \text{ mS cm}^{-1}$ , yielding charge relaxation times of the order of  $5 \text{ ns}$ – $1 \mu\text{s}$ . Hence, transient charging effects might play a role in near interfacial space charge structures. While detailed investigations of transient plasmas interfacing with liquids have been performed, their focus is often on plasma-induced chemistry, and the study of the near interfacial space charge structures remains limited.

Morrow *et al.* modeled the application of transient electric fields to saline solutions to investigate the formation of a liquid double layer ion sheath (although for much smaller voltages than are pertinent to PDSE).<sup>49</sup> For applied voltages of  $10$ – $175 \text{ mV}$  between an electrode and a saline solution, double layers formed on time scales of  $\sim 0.1$ – $110 \mu\text{s}$  for concentrations between  $0.001$  and  $1.0 \text{ M}$ . Shirafuji *et al.* used the same modeling approach for a solution in a system where the metal electrode is replaced by a DBD.<sup>50</sup> While the reaction scheme in the model is simplified, those reactions that were included are representative of the dominant reactions in an aqueous salt solution. The results show that in spite of the  $500 \text{ V}$  drop across the interelectrode gap, the voltage drop across the solution during electron or ion injection is on the order  $-1.3$  and  $2.2 \text{ V}$ , respectively, which is similar to typically applied voltages in conventional electrolysis (see Fig. 4).

Due to the polar nature of water, structural regularity of the liquid is enhanced in the presence of large electric fields. Even though an electric field of  $10^4 \text{ kV cm}^{-1}$  is needed<sup>35</sup> to induce this structure (which is well above plasma-induced electric fields), Dewan *et al.* showed through molecular dynamics simulations that when charge is applied on the surface of an ionic salt solution, water molecules show a net polar ordering. This was attributed to adsorption of positive ions onto the surface.<sup>51</sup> The orientation of water molecules at charged surfaces was also shown to be strongly dependent on the identity of the cations; however, the interfacial ordering depth persists to  $\sim 1 \text{ nm}$ .<sup>51</sup> How this translates to a plasma–liquid interface remains a subject for further investigation. Nonetheless, the gas phase negative space charge region at a liquid anode solution and possible transient surface charging will likely similarly induce a liquid phase double layer.

## 3. Perspective

The structural, chemical, and energetic properties of the reactive interfacial species in PDSE can be significantly influenced by the presence of strong electric fields. The limited modeling studies performed to date may suggest that the structure of a plasma–liquid interface is consistent with an EDL, as found in conventional electrolysis. These findings are based on continuum approaches as there is a lack of state-of-the-art atomistic first-principle approaches of the type that have been applied in conventional electrolysis.<sup>52</sup> Experimental verification is also needed. It remains to be seen how the EDL structure in conventional electrolysis would differ, if at all, from PDSE processes, possibly driven with a significant overvoltage. Such conditions might lead to significant electric field penetration and charge deposition within the solution, particularly when ionization waves are colliding with the liquid surface contributing electric fields in the range of tens to hundreds of  $\text{kV cm}^{-1}$ .<sup>53</sup>

## D. How does plasma impact the solvation structure and dynamics near the plasma-liquid interface?

### 1. Motivation

The interaction of gaseous plasma with liquid surfaces generates exceptionally large fluxes of photons, electrons, ions, and radical species to and through the liquid surface and generates substantial electric fields in the plasma-liquid interfacial region. The changes produced in the structure of the water-air interface by a plasma in contact with the liquid are unknown. Current plasma-liquid interaction models sometimes assume immediate solvation of electrons upon entry in the liquid; yet, it is unclear how the plasma-impacted interfacial layer may influence the solvation dynamics.

### 2. State-of-the-art

Medders and Paesani performed molecular dynamics calculations to simulate vibrational sum frequency generation (VSFG) spectroscopy from a pure water interface (see Fig. 5).<sup>54</sup> The results can be interpreted in terms of a dangling OH stretch mode as well as lower energy features that reflect non-dangling OH stretches

coupled by hydrogen bonds to other water molecules. The results are in good agreement with recent experiments.<sup>54</sup>

Kondo *et al.* used VSFG to characterize a water interface when exposed to a DBD in air.<sup>55</sup> The results indicated that the well-known infrared (IR) peaks associated with H<sub>2</sub>O at the interface (see Medders and Paesani<sup>54</sup>), including the free OH stretch at 3700 cm<sup>-1</sup>, largely disappear after exposure to the plasma (on a time scale of seconds). These features do not reappear until well after the plasma is turned off. They suggest that neutral species from the DBD [e.g., O<sub>2</sub>(<sup>1</sup>D), O<sub>3</sub>, OH, H<sub>2</sub>O<sub>2</sub>, HNO<sub>3</sub>, NO<sub>2</sub>, NO<sub>3</sub>, NO, and N<sub>2</sub>O] react with the surface water, leading to the loss of the IR signal.<sup>55</sup> The effects of electric fields and UV radiation were considered to be unimportant to this phenomenon. While a valuable result, the random nature of micro-discharges in DBDs leads to temporal and spatial averaging of the plasma-induced effects. It may be challenging to identify plasma-induced effects in this type of experiment.

There is uncertainty as to whether there are stable hydrated electron states at the water/air interface. Long-lived states (16 s) are known to exist for electrons at the surface of amorphous solid water.<sup>56</sup> For small liquid water clusters (tens of molecules), the

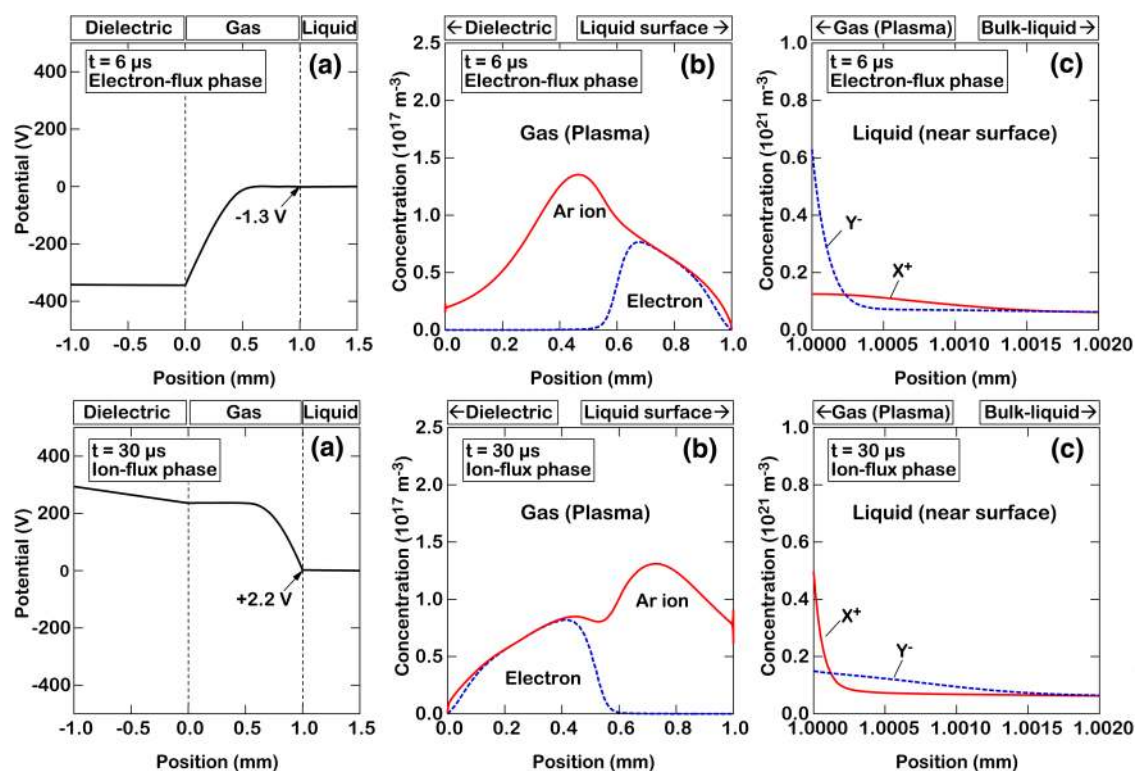


**FIG. 4.** Model of the EDL induced by an AC driven moderate voltage DBD in Ar with a gap of 1 mm impinging on a solution with charge carrier density of  $\sim 0.6 \times 10^{20} \text{ m}^{-3}$ . One of the barriers is a liquid layer. The DBD is driven with 500 V and 20 kHz, and has two current peaks during the cycle. Electron injection occurs at  $6 \mu\text{s}$ . The potential (a), and electron and ion density in the gas phase (b), and liquid phase (c) are shown in the upper three images. The corresponding data at  $30 \mu\text{s}$  when the ion flux is injected in the liquid are shown in the lower three images. The images for different polarity were reported in different figures in the original work and hence the corresponding subfigures have the same subfigure labels. Reprinted with permission from Shirafuji *et al.*, *Jpn. J. Appl. Phys.* **53**, 03DG04 (2014). Copyright 2014 The Japan Society of Applied Physics.



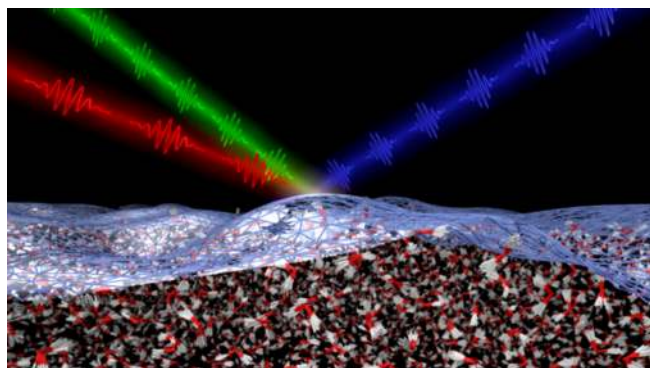


**FIG. 5.** VSGF studies of air-water interface. In VSGF, an infrared laser beam (red beam) is mixed with a visible beam (green beam) producing an output at the sum frequency (blue beam). Reprinted with permission from Medders and Paesani, *J. Am. Chem. Soc.* **138**, 3912–3919 (2016). Copyright 2016 The American Chemical Society.

lowest energy states are on the surface. However, for larger clusters, there are multiple isomers that include surface and bulk-like states.<sup>57</sup> On a flat water interface, calculations indicate that the surface state decays in 1–10 ps to a bulk state.<sup>57</sup> Plasma modeling indicates that solvated electrons react with water 10–20 nm from the surface to produce  $\text{OH}^-$  and  $\text{H}_2$ .<sup>6</sup> Sagar *et al.* studied the solvation of electrons produced by detachment of  $\text{I}^-$  at an air-water interface, experimentally showing that interfacial electron solvation dynamics are similar to those in the bulk liquid.<sup>58</sup> The solvated electrons remain near the interface for more than 750 ps and hence are important reagents in any chemistry occurring within the interface. Rumbach *et al.* estimated, based on non-surface specific absorption measurements and models, that the plasma-produced density of solvated electrons can be  $\sim 1 \text{ mM}$  ( $6 \times 10^{17} \text{ cm}^{-3}$ ) with a penetration depth of  $\sim 2.5 \text{ nm}$ .<sup>5</sup> The measured absorption spectrum was blueshifted by  $\sim 50 \text{ nm}$  from the spectrum typically observed for bulk solvated electrons at room temperature, which suggests some possible divergent properties of the interfacial solvated electrons compared to bulk solvated electrons.

There is a propensity for enrichment of polarizable anions (like  $\text{I}^-$ ) and depletion of cations at aqueous interfaces,<sup>59,60</sup> This behavior is related to the Hofmeister series<sup>61</sup> and has been the subject of numerous molecular dynamics studies as well as experiments. There have not been studies of the influence of plasmas on the interfacial densities of such ions. Tachibana and Yasuoka used this tendency to have an enrichment or decrease of halide ions depending on their polarizability to probe the reaction region produced by a plasma (see Fig. 6).<sup>62</sup> They used  $\text{I}^-$ ,  $\text{Br}^-$ , and  $\text{Cl}^-$ , with  $\text{Cl}^-$  being less likely to be present at the interface compared to the other ions.<sup>63</sup> They found that the average production rates of bromine and iodine were significantly larger than those of chlorine under identical reaction conditions.<sup>62</sup> The authors suggested that reactions at the topmost layer of the solution, approximated to be a molecular monolayer, would be important. A comparison between the plasma treatment and conventional electrolysis showed that chlorine was only evolved in conventional electrolysis while iodine was generated for both PDSE

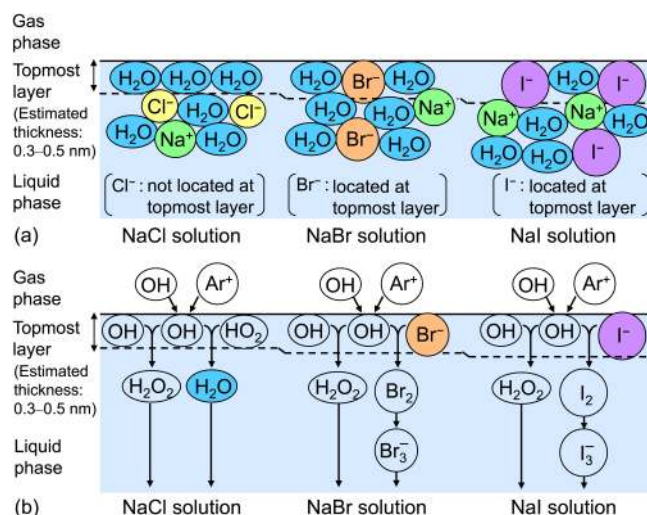


**FIG. 6.** (a) Proposed arrangements of water molecules, sodium, and halide ions at the gas-liquid interface for sodium chloride (NaCl), bromide (NaBr), and iodide (NaI) solutions. (b) Proposed chemical reactions induced by short-lived active species generated by plasma at the gas-liquid interface for NaCl, NaBr, and NaI solutions. Reproduced with permission from Tachibana and Yasuoka, *J. Phys. D: Appl. Phys.* **53**, 125203 (2020). Copyright 2020 IOP Publishing.

and conventional electrolysis. It was suggested that this difference is due to significantly higher electric fields in the EDL at a solid electrode that may not be present at the plasma-liquid interface. These high electric fields are suggested to significantly impact the concentration distribution of ions less likely to be present near the interface, i.e.,  $\text{Cl}^-$ . While further investigations are needed, these results do hint at possible key differences in the solvation structure or EDL between conventional electrolysis and PDSE.

### 3. Perspective

There is very little definitive understanding of the composition and structure of plasma-water interfaces, which means there are many opportunities for molecular-level studies in this area. Many energetic species can enter the water that, together with radical-radical recombination reactions, might lead to a significant localized energy deposition. Several eV of energy can be released in these processes, which is significantly higher than the energy of a hydrogen bond between water molecules ( $\sim 0.24 \text{ eV}$ ). This could impact the solvation structure and dynamics of solvated electrons.

## E. Can the large fluxes and correspondingly large densities of reactive species at the plasma-liquid interface lead to liquid phase processes away from equilibrium driven by chemical kinetics?

### 1. Motivation

A distinctive property of low temperature plasmas is that the energy coupling that produces excited states, radicals, and ions mainly proceeds through electrons (although ions may contribute in

the non-neutral sheath regions). The disparity in masses between the lighter electrons and heavier ions leads to energetic electrons compared to the ions, with electron energies up to two orders of magnitude higher than the heavy particles (neutrals and ions). The end result is highly non-equilibrium kinetics. These highly energetic electrons enable substantial molecular dissociation producing radicals at moderate gas temperatures. Dissociative recombination of ions in molecular gases can produce a comparable density of radicals. These radicals then react among themselves and with other species generating products far from the equilibrium implied by the gas temperature. The question is whether this non-equilibrium behavior that is well understood in the gas phase can be extended into the near interfacial layer of the liquid phase in PDSE.

## 2. State-of-the-art

Contact glow discharge electrolysis (CGDE) is an operating regime of an electrolytic cell at current densities that lead to the formation of a vapor layer around the electrode submerged in the electrolyte solution and the generation of plasma in that vapor layer at increasing voltages.<sup>2</sup> CGDE has many similarities with PDSE, although it is limited to continuous discharge operation in water, which leads to significant heat generation and the production of radicals such as O, H, and OH in the vapor phase.<sup>2</sup> CGDE can be generated at both the anode and the cathode, referred to as anodic and cathodic CGDE. Both operational modes have been shown to generate highly non-Faradaic effects (i.e., processes not induced by electron transfer) that enable the generation of products and product yields that are not attainable by conventional current-mediated electrolysis. Examples of products that have been found in excess of 100% Faradaic efficiency (i.e., the efficiency in which electrons are transferred or utilized in a electrochemical reaction) for anodic CGDE includes H<sub>2</sub>O<sub>2</sub>, Fe<sup>3+</sup> (from Fe<sup>2+</sup>), oxalic acid from formic acid, and N<sub>2</sub>H<sub>4</sub> from aqueous solutions of ammonia. Similarly, non-Faradaic efficiencies for cathodic CGDE were found for I<sup>-</sup> oxidation, and H<sub>2</sub> and O<sub>2</sub> formation.<sup>2</sup> These findings have been attributed to radical-induced reactions.<sup>2</sup> The same effect has been identified in glow discharges in argon with a liquid electrode.<sup>64</sup> It is presently unknown, however, to what extent liquid phase processes may contribute to these effects.

Measurements in a DC-driven glow discharge with a solution cathode have enabled OH densities up to 10<sup>17</sup> cm<sup>-3</sup> (see Ref. 39) leading to OH radical fluxes to the liquid on the order of 10<sup>21</sup> cm<sup>-2</sup> s<sup>-1</sup> while electron fluxes were in the range of 10<sup>18</sup>–10<sup>19</sup> cm<sup>-2</sup> s<sup>-1</sup>.<sup>40</sup> Heat fluxes from the plasma into the liquid can produce significant evaporation from the interface. Using a heat flux balance, an evaporation flux of water vapor into the plasma of ~10<sup>21</sup> cm<sup>-2</sup> s<sup>-1</sup> can be estimated.<sup>40</sup> These are exceptionally large bi-directional fluxes particularly when considering that in electrolysis of water for H<sub>2</sub> evolution, current densities are kept below 1 A cm<sup>-2</sup> (corresponding to an electron flux of 10<sup>19</sup> cm<sup>-2</sup> s<sup>-1</sup>).<sup>65</sup> These large fluxes not only underline the importance of radicals in liquid phase chemistry but also highlight the highly dynamic nature of the plasma–liquid interface. Recently, Oinuma *et al.* quantitatively demonstrated that the oxidation of formate in a droplet can be completely accounted for by the flux of OH radicals from the plasma to the liquid phase.<sup>66</sup> These results show that fluxes of gas phase radicals,

possibly augmented by photolysis, can play a significant role in PDSE in addition to conventional charge-driven Faradaic reactions.

A well-known technique to promote reaction products that are non-energetically favorable in equilibrium conditions is to tune the quenching of radicals by rapidly reducing the gas temperature after the gas has been dissociated by a high-density plasma.<sup>67</sup> This is typically performed by expansion of the plasma. A similar stabilization effect has been suggested for the production of H<sub>2</sub>O<sub>2</sub> in plasmas through which a water spray is applied.<sup>68</sup> While large Henry's law constant for H<sub>2</sub>O<sub>2</sub> does favor the transfer of gaseous H<sub>2</sub>O<sub>2</sub> into the droplets, kinetic effects of enhanced H<sub>2</sub>O<sub>2</sub> production due to radical recombination in the liquid near the plasma–liquid interface has received little attention.

In addition to the extensively studied OH chemistry, plasmas produce a broad range of reactive nitrogen species including peroxy-nitrite as shown in (see Fig. 7).<sup>69</sup> Peroxynitrite chemistry has been shown to produce OH and NO<sub>2</sub> radicals whose presence has been indirectly measured through the detection of nitrated and nitrosylated products of phenol, which are partly responsible for the bactericidal properties of plasma activated water.<sup>70</sup> In addition to nitrogen-oxide chemistry, PDSE in N<sub>2</sub> enables the reduction of N<sub>2</sub> into NH<sub>3</sub> as mentioned in the Introduction.<sup>12</sup>

Enhanced reaction rates and product yields during plasma–liquid interactions as compared to more conventional processes have also been reported for gold nanoparticle synthesis in a plasma-droplet reactor<sup>12</sup> and virus inactivation in aerosol form.<sup>71</sup> The advantage of the generation of plasma at the liquid interface has also been suggested to play a key role in the decomposing perfluorooctanoic acid.<sup>10</sup> All of these examples suggest the importance of the near plasma–liquid interface in PDSE with a strong involvement of charged species or radicals. This non-equilibrium mixture of radicals and charges at the plasma–liquid interface has some resemblance to the reactive surfaces observed in the accelerated chemistry in micro-droplets as demonstrated by Banerjee *et al.*<sup>72</sup>

## 3. Perspective

While non-Faradaic effects of PDSE have been reported with respect to the nature of the products and their yields, it is important to identify whether these effects are only due to gas phase/interfacial processes or whether liquid phase reactions can significantly contribute to these non-Faradaic effects. It remains to be seen whether one can stimulate non-equilibrium reactive chemistry in the solution that is kinetically distinct from the chemistry due to injected gas phase species. It is also untested if this non-equilibrium behavior transferred from the plasma into the liquid can be leveraged to generate recombination products in solution that are otherwise energetically unfavorable.

## IV. WHAT ARE THE FUNDAMENTAL DIFFERENCES BETWEEN PDSE AND OTHER MORE TRADITIONAL ELECTROCHEMICAL PROCESSES?

**A. What is the relative importance of electron, ion, radical, and photon-induced processes in PDSE and to what extent can each be separately controlled?**

### 1. Motivation

While plasmas can produce exceptionally large fluxes of reactive species to a surface, plasmas may consist of tens to hundreds of

different species that may involve hundreds to thousands of reactions.<sup>73–75</sup> As discussed above, electrons, ions, radicals, and photons can influence PDSE individually and possibly collectively leading to significantly more complex chemistry compared to the electron exchange interactions at solid electrode surfaces in conventional electrolysis. It is currently not clear what the relative importance of these different processes is and to what extent they can be leveraged to control PDSE.

## 2. State-of-the-art

Until recently, two different high-level theories explaining plasma-induced liquid chemistry dominated the field. In the context of organic chemistry, the plasma was often considered an example of an advanced oxidation technology and interpreted as a source of OH radicals and to some extent O<sub>3</sub> for plasmas generated in air and O<sub>2</sub>.<sup>76–78</sup> Researchers who approached the field from an electrolysis and conventional CGDE perspective postulated that electron-induced processes dominate, although in many cases the role of radicals that enabled non-Faradaic yields was recognized.<sup>2</sup> The assumption that electron-induced processes dominate was later extended to PDSE involving gas phase glow discharges interacting with metal salt solution electrodes. Electron-induced reduction of metallic ion precursors has consistently been regarded as the dominant mechanism enabling nanoparticle synthesis in these systems. Examples of quantitative analysis of OH and electron dominated process include the decomposition of formate in a droplet in a He–H<sub>2</sub>O RF-driven plasma by OH radicals<sup>66</sup> and the reduction of Ag<sup>+</sup> for a glow discharge in Ar with liquid anode.<sup>79</sup> In the latter case, it was shown that the simultaneous presence of solvated electrons and OH radicals can significantly impact the net amount of reduced Ag<sup>+</sup> due to there being competing reactions (see Fig. 8).<sup>79</sup>

More recently, other plasma-produced gas phase species were identified that can drive important liquid phase processes. These reactions include peroxyxynitrate induced chemistry,<sup>70</sup> O<sub>2</sub>(a<sup>1</sup>Δ) induced inactivation of virus in solutions,<sup>80</sup> the important role of O atoms in forming OCl<sup>–</sup> in saline solutions,<sup>81,82</sup> and enabling direct reactions with hydrocarbons.<sup>83</sup> Many experimental and modeling reports indicate that the reaction pathways can be highly dependent on the plasma configuration and conditions,<sup>1</sup> and in many cases, the relative importance of the possible different reaction pathways remains unclear. Plasmas used to study the interaction with liquids span a range of electron densities of more than six orders of magnitude and can operate at gas temperatures between 300 and 5000 K, so large differences in the resulting PDSE processes and mechanisms are to be expected.<sup>1</sup> Differences in PDSE can be further enhanced by changing the gas composition and plasma excitation method.<sup>69</sup>

Some of the challenges in quantifying the role of different reaction pathways are related to the general lack of understanding about what governs the rate of individual reactions and processes in PDSE. Furthermore, many of the reaction-inducing stimuli are coupled, which makes it difficult to quantify their roles. Nonetheless, by using spin-trapping, hydrogen and oxygen isotopic labeling, and electron paramagnetic resonance spectroscopy on a plasma–liquid system, Gorbanev *et al.* asserted that the reactive species detected in the liquid samples were formed largely in the plasma gas phase.<sup>84</sup>

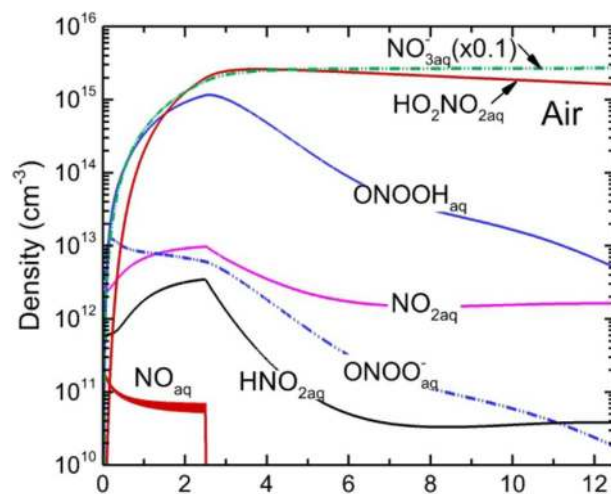


FIG. 7. Reactive nitrogen species produced in a liquid film by a DBD in air as obtained by a 0D model. Many of the reactive nitrogen species have a lifetime of seconds, allowing for transport and are a secondary source of radicals in the bulk liquid. Reproduced with permission from Mohades *et al.*, J. Phys. D: Appl. Phys. **53**, 435206 (2020). Copyright 2020, IOP Publishing.

## 3. Perspective

It is critical to identify how different gas phase plasma conditions impact the resulting PDSE. In view of the complexity of plasma–liquid interactions, it is of key importance to be able to assess the relative importance of the different reaction pathways. While several key reaction pathways have been identified, it remains unclear whether the reported dominant reaction pathways are system specific (or even power dependent in a given system). There is clearly a need to determine for what range of conditions such conclusions can be generalized. The ultimate goal is to distill our description of PDSE to a few dominant reaction pathways. Controlling and fine tuning the generation of individual species and their subsequent reactions will open new directions in PDSE.

### B. What is the PDSE equivalent of manipulating the electrode potential in conventional electrochemistry to enable selective redox processes?

#### 1. Motivation

In conventional electrochemistry, the electrode potential provides fine control of the chemical potential available for redox reactions, making it possible to dictate (for reversible processes) the precise charge of solution species that are exposed to the electrode. The electrode potential is a good descriptor of redox processes and can, for reversible reactions, be directly linked to the decrease in Gibbs free energy per Coulomb of charge transferred (Faraday's law of electrolysis). Hence, the electrode potential is directly linked to the equilibrium constant of the redox reaction, providing a direct connection between charge transfer and equilibrium species concentrations. It is unclear whether there is an



analogous (equivalent) electrode potential that can be used to describe rate kinetics in PDSE.

## 2. State-of-the-art

The electrochemical window of water, the voltage range for which water is neither reduced nor oxidized, is determined by the potentials for the hydrogen and oxygen evolution reactions. The standard potentials are 0 and 1.23 V compared to the standard hydrogen electrode (SHE), respectively. Non-equilibrium effects in PDSE can lead to both reduction and oxidation that occur at potentials well outside the range of conventional electrochemistry. On the reducing side, this would refer to electrons injected into water before they solvate. On the oxidation side, there are numerous plasma species such as OH radicals (2.8 eV) that provide free energies more positive than 1.23 eV. One perspective of PDSE using a liquid anode is that the role of the plasma to produce a high concentration of solvated electrons at the interface. If this is true, the important parameter is the reduction potential of the solvated electron, which is reported to be  $-2.77$  V.<sup>85</sup> This would mean that one can access very reducing conditions not conventionally available in electrochemistry in water. The lifetime of the solvated electron in bulk water is  $\leq 5 \times 10^{-4}$  s,<sup>86,87</sup> which will be further decreased in the presence of scavengers or at low pH through the fast reactions of solvated electrons with  $\text{H}_3\text{O}^+$  or in the presence of high concentrations of solvated electrons favoring the fast second order recombination of solvated electrons.<sup>79</sup> This variable lifetime could significantly impact pulsed PDSE experiments.

It has been demonstrated that plasma electrons can drive electrochemical reduction reactions at the liquid interface. For example, Richmonds *et al.* studied the ferricyanide  $[\text{Fe}(\text{CN})_6^{3-}]$ /ferrocyanide  $[\text{Fe}(\text{CN})_6^{4-}]$  redox couple and found that the rate of reduction of  $\text{Fe}^{3+}$  to  $\text{Fe}^{2+}$  is proportional to the discharge current.<sup>88</sup> However, absorbance measurements of ferricyanide indicated that less than 10% of the injected electrons were involved in reduction. These reactions were further tested in a study by Witzke *et al.* through colorimetric approaches<sup>89</sup> and more recently by Oldham *et al.*<sup>90</sup>

While oxidation and reduction reactions are temporally or spatially separated in conventional electrolytic cells, this is not always the case in PDSE. For example, identical RF plasma conditions have led to both reduction and oxidation reactions at the same location for different chemistries.<sup>91,92</sup> This result might be expected in a low frequency RF-driven plasma in which the changing polarity may produce alternating fluxes of ions, which in water solutions initiate oxidizing reactions, and electrons which produce reducing reactions. Competitive oxidation–reduction processes have also been identified in the modeling of a pulsed DC-driven plasma, shown in Fig. 8. In this system, competitive reactions resulting in the formation of  $\text{AgOH}^+$  and Ag occur as both  $e^-$  and OH radicals are injected from the gas phase.<sup>79</sup>

It was previously noted that plasma electrolysis induced by a gas phase  $\text{N}_2$  plasma enables the synthesis of  $\text{NH}_3$  with a Faradaic efficiency approaching 100%. At the same time, conventional electrochemical reduction of  $\text{N}_2$  for  $\text{NH}_3$  synthesis has been a significant challenge.<sup>93</sup> A recent publication suggests that gas phase production of  $\text{NH}_3$  in the presence of water vapor is equally

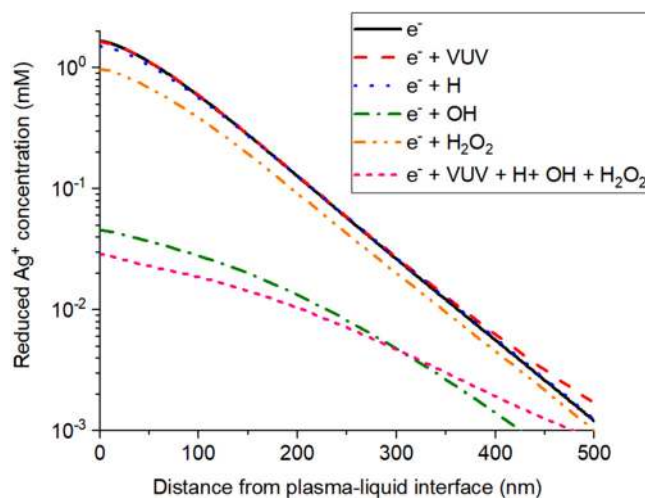


**FIG. 8.** Concentration of reduced  $\text{Ag}^+$  determined by a fluid model for imposed fluxes for typical conditions of an Ar plasma jet impinging on a liquid. Reprinted with permission from Zheng *et al.*, *J. Vac. Sci. Technol. A* **38**, 063005 (2020). Copyright 2020 American Vacuum Society.

efficient as the plasma electrolysis process, if not more so, highlighting the need for a better understanding of the dominant species flux to the solution.<sup>94</sup>

A compelling attempt to link electrochemical potential to PDSE was reported in a recent paper by Oldham *et al.*<sup>90</sup> They report *in situ* measurements of an electrochemical potential in an RF-driven plasma by placing a probe “as close as possible” to the plasma–liquid interface (see Fig. 9). The results showed that for increasing plasma power, an increasing applied overpotential was observed and the corresponding measured reduction reaction rate of indigo carmine and methyl viologen increased as well. While their measured reaction rates trend toward saturation at higher plasma powers, the authors did not observe a saturation of the overpotential. While the interpretation of the measured potential requires further clarification, it does raise questions on what limits the reaction rate of redox reactions in PDSE. In conventional electrolysis, the reduction reaction rate is limited by mass transport and applied overpotential. Similarly experiments performed by Delgado *et al.* showed that insufficient reactant transport can reduce predicted Faradaic efficiencies for PDSE at low reactant concentrations.<sup>95</sup> The typically large radical concentrations at the plasma–liquid interface induce significant radical–radical recombination, which could be a major loss mechanism at higher operational plasma powers, in addition to mass transport limitations. These limits will be further addressed in the next question.

## 3. Perspective

A major question to be addressed in future research is whether control of PDSE is fully determined by gas phase species fluxes in the absence of a work function as at the solid metal–water interface or does the voltage drop across the solution play a



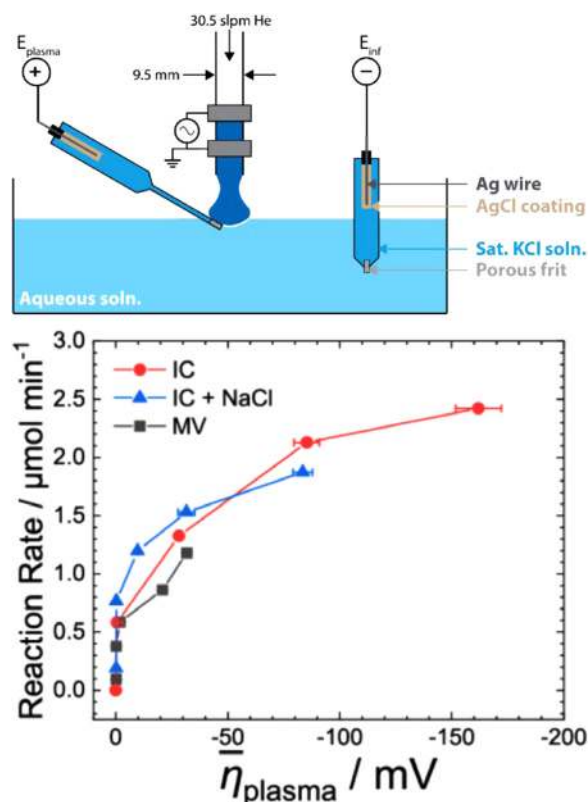


**FIG. 9.** (Upper) Experimental setup including reference electrode in the bulk solution far away from the plasma for electrochemical potential measurements in solution near a RF-driven plasma. (Lower) Reaction rate of plasma-induced indigo carmine and methyl viologen as a function of the measured potential difference between the two electrodes shown in the upper figure. The negative sign indicates reducing conditions. Reproduced with permission from Oldham *et al.*, *J. Phys. D: Appl. Phys.* **53**, 165202 (2020). Copyright 2020 IOP Publishing.

major role? Can this voltage drop be ultimately tuned to drive selective reactions similar to conventional electrochemistry? Or is it more appropriate to think of PDSE with a solution anode as dominantly driven by solvated electrons and occurring at  $-2.77$  V on average, with a broader range of oxidation and reduction processes that arise from minor species and non-equilibrium effects? Equivalently, for a solution cathode, can we think of PDSE as predominantly driven by oxidation reactions induced by OH radicals with a redox potential of  $2.8$  eV?

### C. What are the key differences in transport limited chemical conversion in electrochemistry and PDSE?

#### 1. Motivation

In electrolysis, reactions occur at the surface of a metal electrode. Mass transport of species to the electrode must occur in order for them to react. This requirement leads to the formation of diffusion layers and to a significant extent determines the shape of

voltammograms (current vs applied potential) in cyclic voltammetry.<sup>96</sup> Plasma-liquid interactions involve various chemical phenomena including generation of short-lived active species in the gas phase and transport of these species through the plasma-liquid interface and into the bulk solution. These transport phenomena lead to species gradients in the liquid having length scales ranging from  $10$  nm for electrons to a few micrometers for radicals like OH (depending on the absolute generation rate of OH). In conventional electrolysis, electron-induced reactions will occur at the electrode, as electrons do not penetrate into the solution and reactants need to be transported to the electrode interface. As in conventional electrolysis, species in the bulk solution need to transport into the zones of high plasma-produced solvated electron and radical densities at the surface to enable conversion reactions. PDSE is transport limited as in conventional electrolysis, but inherently more complex as it includes gas phase and radical transport in the plasma-solution boundary layer. The transport of gas phase reactants to the liquid is, compared to transport in the liquid, in principle, more easily controlled by selection of power, excitation method, voltage waveform, and gas mixture. The thicknesses of the solvated electron and radical species transport layers are likely outcomes of plasma transport into the liquid. However, it is not clear that their properties rise to the level of control achievable in the gas phase and how they are coupled with reactant transfer from the bulk solution.

#### 2. State-of-the-art

Multi-phase transfer of reactive species—from plasma to liquid—is transport limited as reaction times, particularly for radical species, are shorter than typical transport time scales. This is a significant challenge for PDSE. Transport of plasma generated reactive species is from the gas phase to the plasma-liquid interface, and subsequently from the plasma-liquid interfacial region into the bulk liquid. Several strategies have been pursued to overcome gas phase transport limits in PDSE by enhancing the surface-to-volume ratio of the solution. This includes producing plasmas in bubbles in the liquid,<sup>97</sup> integrating a plasma source with a microfluidic chip<sup>98</sup> and combining gas phase plasmas with liquid spray/droplets.<sup>99</sup>

In the liquid phase, diffusive transport is significantly slower than in the gas phase and hence is potentially even more limiting than in the gas phase. Several groups have investigated the extent of the reactivity region of the plasma-liquid interface both numerically and experimentally. Takeuchi *et al.* studied the decomposition of acetic acid in aqueous solution when irradiated with an argon plasma.<sup>100</sup> Based on a numerical model, they concluded that OH radicals diffuse into the bulk liquid to a depth of  $\sim 1$   $\mu\text{m}$ . These results were consistent with earlier studies by Hamaguchi *et al.*,<sup>101</sup> who demonstrated that OH radicals supplied to the water from gas phase plasma were present in a thin layer of  $\sim 1$   $\mu\text{m}$  from the plasma-water interface with lifetimes on the order of  $\sim 1$  ms. The authors noted that many short-lived species remain close to the gas-liquid interface rather than moving into the bulk. This has been shown to lead to diffusion-limited OH-induced reactions in a plasma-droplet study (see Fig. 10)<sup>66</sup> and convection limited radical-induced reactions in a plasma jet-liquid interaction study.<sup>102</sup> Similar conclusions can be drawn for PDSE enabled by

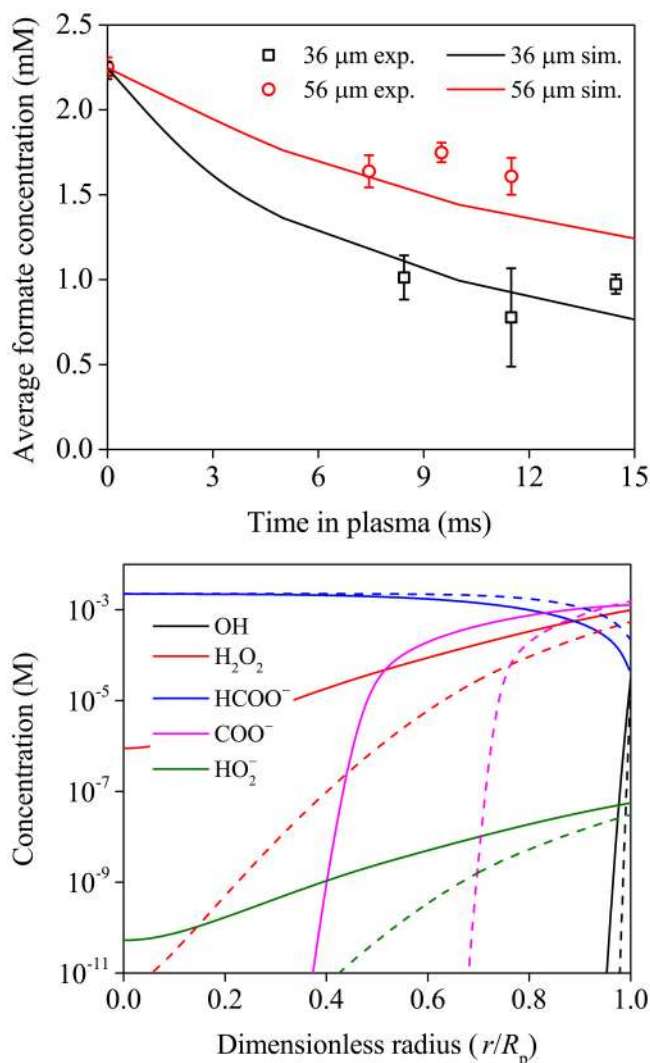


**FIG. 10.** (Upper) Comparison of the decomposition of formate in a droplet exposed to a He–H<sub>2</sub>O diffuse glow discharge as obtained with a 1D reaction diffusion model with equivalent experimental measurements. (Lower) Radial profile of dominant species in a droplet after 10 ms in the plasma for droplet diameters of 36 μm (solid line) and 56 μm (dashed line). The formate is decomposed by OH present at concentrations in excess of 10 μM in a layer with thickness of ~2 μm. A depletion of the formate concentration near the plasma–droplet interface enables diffusion of formate into the layer with abundant OH radicals and subsequent formate decomposition. Reproduced with permission from Oinuma *et al.*, *Plasma Sources Sci. Technol.* **29**, 095002 (2020). Copyright 2020 IOP Publishing.

electrons.<sup>79,103</sup> Similarly to electrons at the plasma–solution anode interface, ion penetration might be important at the plasma–solution cathode interface. While energetic ions can penetrate the liquid surface (see above) and may produce sputtering of H<sub>2</sub>O molecules, in many cases, charge exchange will lead to the

production of H<sub>3</sub>O<sup>+</sup>, an ion already present in water. This likely results in a pH gradient near the interface. Gradients in solution phase ion densities near the plasma–liquid interface can be impacted by both ion drift and diffusion. In the case of PDSE, electric field penetration, possibly due to transient surface charging of the liquid interface, might impact solution phase charged species gradients significantly near the plasma–solution interface.

### 3. Perspective

It is necessary to investigate the effect of gradients and penetration depths of short-lived species near the plasma–liquid interface in a more controlled fashion and for a broader range of species. Such studies could greatly benefit from homogeneous plasma–liquid interaction conditions and controlled liquid volumes that could include droplets or continuous-flow microfluidics reactors for which the effect of convection on time scales of interest can be limited or externally controlled.

## D. Are current models capable of quantitatively describing the fundamental PDSE processes?

### 1. Motivation

There are at least two classes of models relevant to PDSE. The first is molecular-level models that use classical, quantum, and statistical mechanics to determine rates, structures, thermodynamic properties, and non-equilibrium effects relevant to PDSE. The second is plasma chemistry models that describe species, concentrations, reactions, material, and thermal transport subject to known reaction rates, and thermodynamic and structural properties. To date, the transfer of species from the gas to the liquid phase and vice versa in plasma–liquid interaction models does not include as much rigor as found in state-of-the-art aerosol models,<sup>104</sup> which are specialized to study this very phenomenon. Due to their more comprehensive approach, plasma chemistry models that include reactor scale processes, plasma generation, Poisson’s equation, reaction kinetics (gas phase and liquids), and gas–liquid and radiation transport generally have a simplified description of the interfacial region, which may not include some of the non-equilibrium aspects described above. The impact of these simplifications remains unclear.

### 2. State-of-the-art

There are comprehensive models of non-equilibrium plasma and of liquid phase chemistry, although only a few models merge both aspects.<sup>1</sup> Several models have been developed for plasmas directly in liquids or bubbles.<sup>105–108</sup> Similar models exist for sonoluminescence in which hydrodynamics are simultaneously modeled with chemistry.<sup>109</sup> However, these models likely do not have the spatial resolution required to address the physical and chemical processes at the plasma–liquid interface to the level of detail discussed here. Advanced global and multi-dimensional models of plasmas interacting with liquids have been developed.<sup>50,110–112</sup> These models include detailed studies of plasma jets and DBDs interacting with a liquid layer involving reactivity transfer from the gas to the liquid phase. An example is shown in (see Fig. 11).<sup>113</sup> In addition, other research groups have addressed DC glow discharges<sup>100</sup> and RF discharges<sup>114</sup> in contact with liquids. Plasma

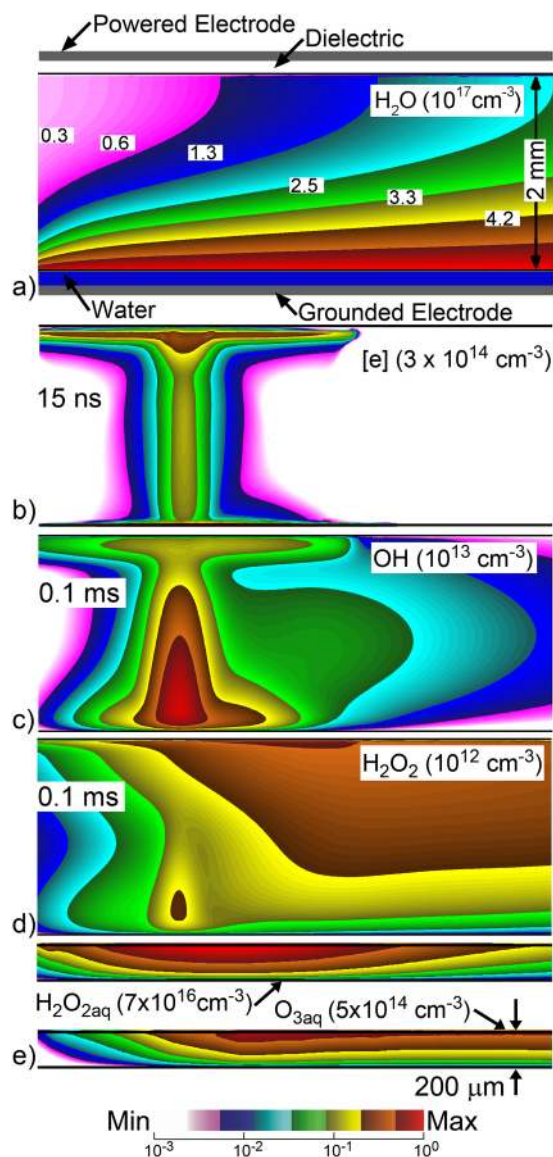


**FIG. 11.** Results from modeling of a DBD over a thin water layer with air flow from left to right. (a) Water vapor evaporating from the liquid, (b) electron density after the 15 ns discharge pulse, (c) OH, and (d)  $\text{H}_2\text{O}_2$  0.1 ms after the discharge pulse while convecting downstream. (e)  $\text{H}_2\text{O}_2$  and  $\text{O}_3$  in the  $200\text{ }\mu\text{m}$  thick liquid layer.<sup>113</sup> The values are plotted over three decades with the maximum value indicated in the image, except for the water vapor, which is on a linear scale with contour labels in units of  $10^{17}\text{ cm}^{-3}$ . For the gas phase plots, the full geometry is shown for  $\text{H}_2\text{O}$ . For the other images, the upper and lower boundary of the figure are the dielectric and the liquid interface, respectively. Reproduced with permission from Tian *et al.*, *Plasma Sources Sci. Technol.* **25**, 055020 (2016). Copyright 2016 IOP Publishing.

chemical reaction mechanisms are available for building both gas and liquid phase kinetics models.<sup>1,74,115–119</sup> Given the more comprehensive nature of these models in terms of processes included and dynamic range, as discussed in Sec. IV D 1, the transfer of

species from the gas to the liquid phase and vice versa in plasma–liquid interaction models do not have the level of detail as in state-of-the-art aerosol models.<sup>120,121</sup>

The plasma–liquid interface in these detailed plasma kinetic models that describe the entire plasma–liquid reactor system have to date not had the spatial and time resolution required to address many of the transport challenges discussed above. In principle, these models contain the pertinent physics and transport (i.e., nonequilibrium mass, momentum, and energy equations coincident with solution of Poisson’s equations) to address these processes. What these models currently lack is the ability to resolve a dynamic range of sub-nm to tens of cm, and sub-ps to many seconds. In conventional fluid models that resolve chemical kinetics and transport in both the gas and liquid phase even with scale lengths as small as tens of micrometers, the plasma–liquid interface is treated as a boundary with algorithms to limit transport to and from the boundary. While the science is largely understood and extensive studies have been reported on mass accommodation,<sup>122</sup> key data are lacking for important reactive species and might require significant assumptions even in state-of-the-art models.

Simulations in the gas phase have shown that the near interfacial densities can depend on the reactive sticking coefficient of radicals at the surface even at atmospheric pressure.<sup>123</sup> In this context, reactive sticking coefficient refers to the probability that the radical leaves the gas phase when striking the liquid. Lindsay *et al.* showed that for a fully coupled description of the plasma–liquid interface, the electron density and energy near the plasma–liquid interface strongly depends on the chosen reactive sticking coefficient.<sup>124</sup> This could impact the energy of electrons injected into the liquid, at least if electrons have a non-unity reactive sticking coefficient. Given the nanometer length scale of the EDL, it is not likely that both the EDL and reactor scale processes can be self-consistently included in a single numerical mesh. However, these scale lengths may be included by using an analytical boundary layer model similar to those used for sheaths in conventional gas phase plasma simulations when the sheath is not spatially resolved.<sup>125</sup> Note that a molecular understanding of EDLs at the interface of a solid electrode in contact with liquid remains an active subject of research.<sup>52,126</sup>

To gain further understanding of the interfacial layer, a focus on the near interfacial region with nanometer resolution might be valuable. In this case, one could even step away from considering the plasma–liquid interface as a boundary and use density profile functions to gradually change from the gas to the liquid phase within a continuum. Garland *et al.* recently conducted a comparative study of models for electron transport across such density gradient profiles representing an Ar–liquid interface.<sup>127</sup>

At the level of molecules (ions and electrons) interacting with a water slab or cluster, molecular dynamics, sometimes including trajectory surface hopping, can provide significant information about rate processes that is adequate for predicting and interpreting experiments. Examples of molecular dynamics simulations to calculate sputtering processes and sputtering yields (as shown in Fig. 3) can, for example, provide sputtering yields that can be incorporated into the boundary conditions of a multi-phase plasma model.



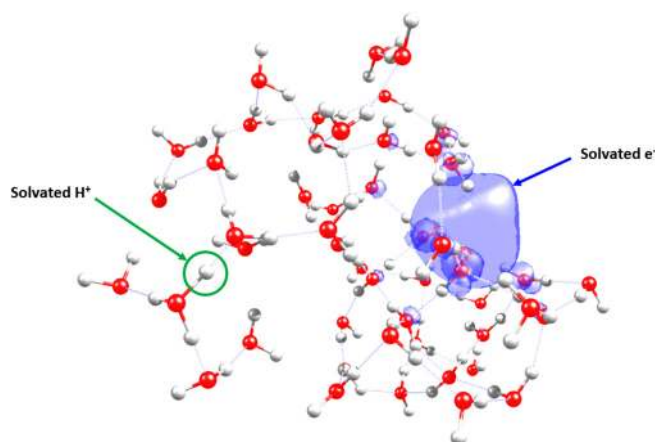


**FIG. 12.** Fragment of a Born–Oppenheimer molecular dynamics trajectory simulating the recombination of a solvated proton and a solvated electron in a water cluster containing 35 water molecules. The solvated electron is mostly localized on the surface of the cluster at a distance over 5 Å from the proton, and the structure is stable for about 1 ps. Shorter distances enable recombination at sub-picosecond time scales, but larger distances lead to activated recombination kinetics with much longer time scales (unpublished work from L. Jones and G. Schatz).

A limitation of molecular dynamics simulations is with their use of empirical force fields, which are adequate for nonbonding interactions and for times up to microseconds. However, the treatment of reactions requires electronic structure calculations on the fly (Fig. 12), and this limits times for direct simulation of dynamic processes to 100 ps. For longer time scales, rate processes must be described in terms of reaction barriers and transition state theory. However, electronic structure calculations have limitations on accuracy such that one cannot determine reaction barriers and related dynamical properties with the precision required for chemical kinetics.

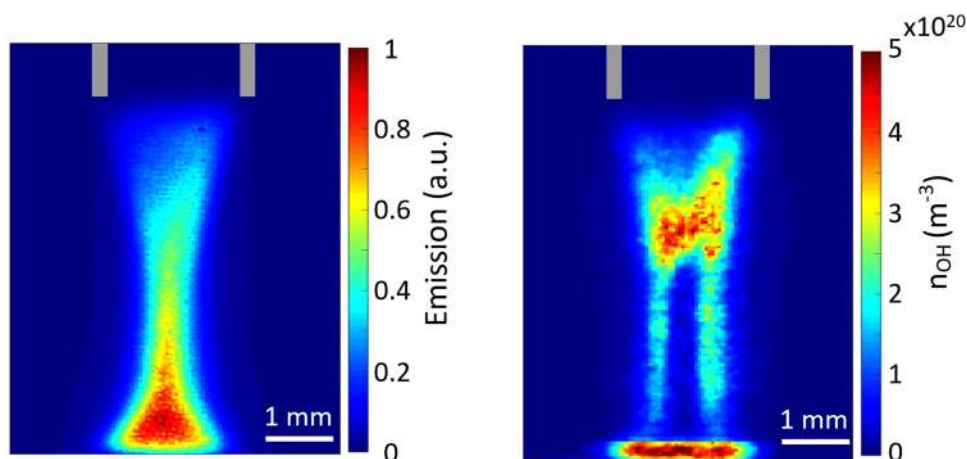


**FIG. 13.** Optical emission intensity and corresponding OH density distribution in a plasma jet operating in He–H<sub>2</sub>O and impinging on a saline solution. The OH density is obtained by planar laser induced fluorescence. The plasma–liquid interface corresponds to the bottom boundary of the image. The maximum OH density is found near this plasma–liquid interface (unpublished work from Yue and Bruggeman).

### 3. Perspective

Both molecular and reactor scale (plasma–liquid) models have limitations with respect to the dynamic range that they are able to address. These limitations at some point affect the accuracy of their predictions. Given the practical limitations on the accuracy of molecular-level theory, one strategy to improve accuracy is to iterate between theory and experiment to determine molecular-level properties. There needs to be iteration and sensitivity studies between molecular and plasma chemistry models to identify key unknowns whose values need to be determined. In addition, plasma chemistry models should also be validated by experiments. This calls for a strongly integrated research program combining modeling and experimental activities to tackle this challenge.

## E. What are the optimal methods to quantify the fundamental PDSE processes experimentally?

### 1. Motivation

Liquid phase chemistry in PDSE can lead to a complex mixture of short- and long-lived aqueous reactive species. Determining the composition of these reactive species and intermediates at the interface may enable identifying dominant PDSE reaction pathways and possibly lead to insights into how to control PDSE. Short-lived species require *in situ* and fast measurements. Performing these measurements presents challenges particularly in the near interfacial plasma–liquid layer in the presence of large concentration gradients and electric fields. The exceedingly small length scales of interest ranging from a few nanometers to a few micrometers also present challenges. On the scale length of, for example, the EDL, the liquid surface is not flat and quiescent. These dynamics of the interface present challenges to diagnostics to produce meaningful spatially and time-resolved measurements, as opposed to averages over these dynamics.

### 2. State-of-the-art

Diagnostics that can contribute to an enhanced understanding of PDSE involve both the measurement of fluxes of gas phase



species to the liquid and species present in the solution.<sup>1</sup> The integrated flux of injected electrons can be measured through conduction current measurements, which may be a significant challenge in highly transient plasmas.<sup>128</sup> While species fluxes to solid surfaces can be measured through molecular beam mass spectrometry,<sup>129</sup> the limited accessibility of the plasma–liquid interface requires alternative techniques. Spatial gas phase electron density distributions and electron temperature measurements can be made by Thomson scattering.<sup>130</sup> Radical species fluxes, such as H<sup>•</sup> and <sup>•</sup>OH can be measured by laser induced fluorescence or absorption techniques.<sup>131–133</sup> An example is shown in Fig. 13. All of these techniques are well established, although challenges remain to resolve species gradients at the plasma–liquid interface, which have (sub-)micrometer scale lengths, conditions that are further complicated by the deformable liquid interface.

There are many methods to probe the composition of solutions based on optical spectroscopy, electron paramagnetic resonance spectroscopy, and mass spectrometry.<sup>134–136</sup> The majority of these techniques have been mainly used for the detection of long-lived species or through turn-on colorimetric and spin-trapping to produce changes in longer-lived species that directly relate to the short-lived intermediates. For example, broadband UV/Vis absorption spectroscopy is extensively used for the measurement of long-lived species generated by PDSE. Examples include the characterization of OCl<sup>-</sup>, NO<sub>3</sub><sup>-</sup>, NO<sub>2</sub><sup>-</sup>, H<sub>2</sub>O<sub>2</sub>, and dissolved oxygen species.<sup>81,137</sup>

While these approaches have led to major analytical chemistry advances, the complexity of PDSE makes the quantitative interpretation of indirect measurements challenging. This complexity results from the non-trivial mixture of short-lived and long-lived aqueous reactive species. This is particularly the case in the near interfacial plasma–liquid layer in the presence of large concentration gradients with many possible competing reactions and transport limits. Solvated electrons have been measured in bulk solution in the field of radiolysis by optical absorption and by non-linear optical techniques at liquid–water interfaces.<sup>58,138</sup> The only measurements performed at the plasma–liquid interface are line-integrated solvated electron density measurements by total internal reflection with weak absorbance of the order of 10<sup>-5</sup>, as shown in Fig. 14.<sup>5</sup> While measurements of bulk solution properties are available for PDSE and several reaction pathways have been identified, the majority of the information is based on indirect measurements through long-lived species or the introduction of specific scavengers.<sup>1</sup>

Identifying the fundamental processes that define PDSE requires experiments that are sensitive to the composition of reactive species (ions, radicals, hot electrons, solvated electrons) and strong electric fields present at the plasma–liquid interface. All the above methods, while extremely valuable, have inherent limitations on selectivity and temporal or spatial resolution.<sup>1</sup>

The majority of diagnostics that are available for gas–liquid interfaces require highly controlled environments to produce unambiguous and reproducible results. These diagnostics include x-ray photoelectron spectroscopy and molecular beam techniques. With the exception of second-harmonic generation (SHG),<sup>55</sup> surface sensitive techniques have not been applied to the plasma–liquid interface to date. Similarly, a broad range of high-resolution diagnostics, although not-surface specific, have

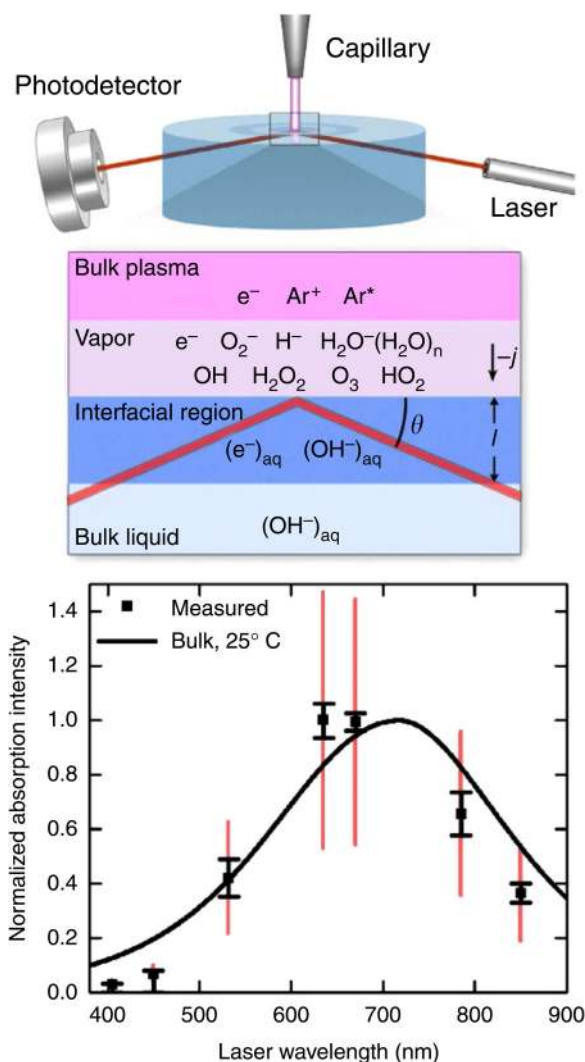


FIG. 14. (Upper) Schematic representation of the total internal reflection tunable diode laser absorption to detect solvated electrons at the plasma–liquid interface. (Lower) Obtained solvated electron absorption spectrum. Reprinted with permission from Rumbach *et al.*, Nat. Commun. 6, 7248 (2015). Copyright 2015, licensed under a Creative Commons Attribution (CC BY) license.

recently enabled *in situ* liquid phase diagnostics, including stimulated Raman spectroscopy and transmission electron microscopy, but they have not yet been extended to *in situ operando* measurements during PDSE.<sup>139,140</sup>

### 3. Perspective

There is a strategic opportunity to leverage diagnostic capabilities developed in other research areas to PDSE to enable high spatial and temporal diagnostics of PDSE-produced species in the liquid phase. A significant challenge impeding implementing

these diagnostics is combining the expertise required by many of these advanced techniques with plasma expertise, as well as interpreting the highly complex signals generated particularly by the optical diagnostics. Interface-selective and electric field sensitive spectroscopic techniques such as SHG and sum frequency generation (SFG) would provide unique insights into the composition and reactivity of the non-equilibrium plasma-liquid interface. However, overcoming large non-resonant contributions from the impinging strong electric fields from the plasma would be a challenge. Nonetheless, initial results suggest that electronic-SFG and vibrational-SFG might serve as important probes of the plasma-liquid interface regarding the orientation of neutral, radical, and ionic species and the formation of electric double layers.

## V. CONCLUSION

While plasma interactions with aqueous solutions to induce chemical modifications have been studied by continuous DC-driven plasmas inspired by electrolysis, and date back to the pioneering work of Gubkin in 1887,<sup>16</sup> a detailed understanding of these exceedingly complex phenomena remains elusive. We have discussed ten important questions for the research field that we believe can be addressed by exploiting recent advances in plasma science and other research areas. While many open questions remain, the large variety of possible processes often makes it challenging to decouple parameters and define dominant reaction and transport mechanisms. A basic understanding is emerging, though often based on correlations and indirect measurements. In view of the complexity and limitations of both modeling and diagnostics, a strong interaction and collaboration between major modeling and diagnostics efforts will be required to enable predictive control of PDSE. This cross-disciplinary engagement has the potential to promote transformational advances in our ability to use plasmas for selective, efficient, green chemical transformations and innovative new materials synthesis, and in doing so develop an additional potent enabling technology for the electrification of the chemical industry.

## ACKNOWLEDGMENTS

Research was sponsored by the Army Research Office and was accomplished under Grant No. W911NF-20-1-0105. The views and conclusions contained in this document are those of the authors and should not be interpreted as representing the official policies, either expressed or implied, of the Army Research Office or the U.S. Government. The U.S. Government is authorized to reproduce and distribute reprints for Government purposes notwithstanding any copyright notation herein. The theory research was supported in part through the computational resources and staff contributions provided for the Quest high performance computing facility at Northwestern University, which is jointly supported by the Office of the Provost, the Office for Research, and Northwestern University Information Technology. This work was also partially supported by the U.S. Department of Energy, Office of Science, Office of Fusion Energy Sciences, under Award Nos. DE-SC0020232 and DE-SC0016053, and the National Science Foundation (Nos. PHY-1902878 and PHYS 1903151).

## DATA AVAILABILITY

Data sharing is not applicable to this article as no new data were created or analyzed in this study.

## REFERENCES

- <sup>1</sup>P. J. Bruggeman, M. J. Kushner, B. R. Locke, J. G. E. Gardeniers, W. G. Graham, D. B. Graves, R. C. H. M. Hofman-Caris, D. Maric, J. P. Reid, E. Ceriani, D. F. Rivas, J. E. Foster, S. C. Garrick, Y. Gorbanev, S. Hamaguchi, F. Iza, H. Jablonowski, E. Klimova, J. Kolb, F. Krcma, P. Lukes, Z. Machala, I. Marinov, D. Mariotti, S. M. Thagard, D. Minakata, E. C. Neyts, J. Pawlat, Z. L. Petrovic, R. Pflieger, S. Reuter, D. C. Schram, S. Schröter, M. Shiraiwa, B. Tarabová, P. A. Tsai, J. R. R. Verlet, T. von Woedtke, K. R. Wilson, K. Yasui, and G. Zvereva, *Plasma Sources Sci. Technol.* **25**, 053002 (2016).
- <sup>2</sup>S. K. S. Gupta, *Plasma Sources Sci. Technol.* **24**, 063001 (2015).
- <sup>3</sup>P. Rumbach and D. B. Go, *Top. Catal.* **60**, 799–811 (2017).
- <sup>4</sup>R. Akolkar and R. M. Sankaran, *J. Vac. Sci. Technol. A* **31**, 050811 (2013).
- <sup>5</sup>P. Rumbach, D. M. Bartels, R. M. Sankaran, and D. B. Go, *Nat. Commun.* **6**, 7248 (2015).
- <sup>6</sup>R. Gopalakrishnan, E. Kawamura, A. J. Lichtenberg, M. A. Lieberman, and D. B. Graves, *J. Phys. D: Appl. Phys.* **49**, 295205 (2016).
- <sup>7</sup>P. Vanraes and A. Bogaerts, *Appl. Phys. Rev.* **5**, 031103 (2018).
- <sup>8</sup>J. E. Foster, *Phys. Plasmas* **24**, 055501 (2017).
- <sup>9</sup>V. Scholtz, J. Pazlarova, H. Souskova, J. Khun, and J. Julak, *Biotechnol. Adv.* **33**, 1108–1119 (2015).
- <sup>10</sup>G. R. Stratton, F. Dai, C. L. Bellona, T. M. Holsen, E. R. V. Dickenson, and S. Mededovic Thagard, *Environ. Sci. Technol.* **51**, 1643–1648 (2017).
- <sup>11</sup>Y. Gorbanev, D. Leifert, A. Studer, D. O'Connell, and V. Chechik, *Chem. Commun.* **53**, 3685–3688 (2017).
- <sup>12</sup>R. Hawtof, S. Ghosh, E. Guarr, C. Xu, R. M. Sankaran, and J. N. Renner, *Sci. Adv.* **5**, eaat5778 (2019).
- <sup>13</sup>P. Maguire, D. Rutherford, M. Macias-Montero, C. Mahony, C. Kelsey, M. Tweedie, F. Pérez-Martin, H. McQuaid, D. Diver, and D. Mariotti, *Nano Lett.* **17**, 1336–1343 (2017).
- <sup>14</sup>S. G. Booth and R. A. W. Dryfe, *J. Phys. Chem. C* **119**, 23295–23309 (2015).
- <sup>15</sup>P. S. Toth and R. A. W. Dryfe, *Analyst* **140**, 1947 (2015).
- <sup>16</sup>J. Gubkin, *Ann. Phys.* **268**, 114–115 (1887).
- <sup>17</sup>F. Rezaei, P. Vanraes, A. Nikiforov, R. Morent, and N. De Geyter, *Materials* **12**, 2751 (2019).
- <sup>18</sup>B. Eliasson, M. Hirth, and U. Kogelschatz, *J. Phys. D: Appl. Phys.* **20**, 1421 (1987).
- <sup>19</sup>Y. Itikawa, *J. Phys. Chem. Ref. Data* **34**, 1 (2005).
- <sup>20</sup>J. Ma, S. A. Denisov, A. Adhikary, and M. Mostafavi, *Int. J. Mol. Sci.* **20**, 4963 (2019).
- <sup>21</sup>B. C. Garrett, D. A. Dixon, D. M. Camaioni, D. M. Chipman, M. A. Johnson, C. D. Jonah, G. A. Kimmel, J. H. Miller, T. N. Rescigno, P. J. Rossky, S. S. Xantheas, S. D. Colson, A. H. Laufer, D. Ray, P. F. Barbara, D. M. Bartels, K. H. Becker, K. H. Bowen, S. E. Bradforth, I. Carmichael, J. V. Coe, L. R. Corrales, J. P. Cowin, M. Dupuis, K. B. Eisenthal, J. A. Franz, M. S. Gutowski, K. D. Jordan, B. D. Kay, J. A. LaVerne, S. V. Lymar, T. E. Madey, C. W. McCurdy, D. Meisel, S. Mukamel, A. R. Nilsson, T. M. Orlando, N. G. Petrik, S. M. Pimblott, J. R. Rustad, G. K. Schenter, S. J. Singer, A. Tokmakoff, L. S. Wang, and T. S. Zwier, *Chem. Rev.* **105**, 355–390 (2005).
- <sup>22</sup>V. Svoboda, R. Michiels, A. C. LaForge, J. Med, F. Stienkemeier, P. Slavíček, and H. J. Wörner, *Sci. Adv.* **6**, eaaz0385 (2020).
- <sup>23</sup>A. Balcerzyk, U. Schmidhammer, F. Wang, A. de la Lande, and M. Mostafavi, *J. Phys. Chem. B* **120**, 9060–9066 (2016).
- <sup>24</sup>M. U. Sander, M. S. Gudiksen, K. Luther, and J. Troe, *Chem. Phys.* **258**, 257–265 (2000).
- <sup>25</sup>A. Balcerzyk, U. Schmidhammer, G. Horne, F. Wang, J. Ma, S. M. Pimblott, A. de la Lande, and M. Mostafavi, *J. Phys. Chem. B* **119**, 10096–10101 (2015).
- <sup>26</sup>J. Meesungnoen, J. P. Jay-Gerin, A. Filali-Mouhim, and S. Mankhetkorn, *Radiat. Res.* **158**, 657–660 (2002).

- <sup>27</sup>N. Ottosson, M. Faubel, S. E. Bradforth, P. Jungwirth, and B. Winter, *J. Electron Spectrosc. Relat. Phenom.* **177**, 60–70 (2010).
- <sup>28</sup>J. Kruszelnicki, A. M. Lietz, and M. J. Kushner, *J. Phys. D: Appl. Phys.* **52**, 355207 (2019).
- <sup>29</sup>A. M. Lietz and M. J. Kushner, *J. Phys. D: Appl. Phys.* **49**, 425204 (2016).
- <sup>30</sup>F. Tochikubo, Y. Shimokawa, N. Shirai, and S. Uchida, *Jpn. J. Appl. Phys.* **53**, 126201 (2014).
- <sup>31</sup>H. Delgado, D. Elg, D. Bartels, P. Rumbach, and D. Go, *Langmuir* **36**(5), 1156–1164 (2020).
- <sup>32</sup>W. A. Donald, R. D. Leib, J. T. O'Brien, M. F. Bush, and E. R. Williams, *J. Am. Chem. Soc.* **130**, 3371–3381 (2008).
- <sup>33</sup>M. F. Russo, C. Szakal, J. Kozole, N. Winograd, and B. J. Garrison, *Anal. Chem.* **79**, 4493–4498 (2007).
- <sup>34</sup>D. J. Levandier, Y. H. Chiu, R. A. Dressler, L. Sun, and G. C. Schatz, *J. Phys. Chem. A* **108**, 9794–9804 (2004).
- <sup>35</sup>Y. Minagawa, N. Shirai, S. Uchida, and F. Tochikubo, *Jpn. J. Appl. Phys.* **53**, 010210 (2013).
- <sup>36</sup>A. Yu. Nikiforov, *High Energy Chem.* **42**, 235–239 (2008).
- <sup>37</sup>N. Y. Babaeva, N. Ning, D. B. Graves, and M. J. Kushner, *J. Phys. D: Appl. Phys.* **45**, 115203 (2012).
- <sup>38</sup>N. A. Sirotkin and V. A. Titov, *Plasma Chem. Plasma Process.* **37**, 1475–1490 (2017).
- <sup>39</sup>Q. Xiong, Z. Yang, and P. J. Bruggeman, *J. Phys. D: Appl. Phys.* **48**, 424008 (2015).
- <sup>40</sup>T. Verreycken, A. F. H. van Gessel, A. Pageau, and P. Bruggeman, *Plasma Sources Sci. Technol.* **20**, 024002 (2011).
- <sup>41</sup>J. Zeleny, *Phys. Rev.* **10**, 1–6 (1917).
- <sup>42</sup>D. Levko, R. R. Arslanbekov, and V. I. Kolobov, *J. Appl. Phys.* **127**, 043301 (2020).
- <sup>43</sup>P. Bruggeman, L. Graham, J. Degroote, J. Vierendeels, and C. Leys, *J. Phys. D: Appl. Phys.* **40**, 4779–4786 (2007).
- <sup>44</sup>P. Bruggeman, J. Degroote, C. Leys, and J. Vierendeels, *J. Phys. D: Appl. Phys.* **41**, 194007 (2008).
- <sup>45</sup>A. J. Schwartz, S. J. Ray, E. Elish, A. P. Storey, A. A. Rubinshtein, G. C. Y. Chan, K. P. Pfeuffer, and G. M. Hieftje, *Talanta* **102**, 26–33 (2012).
- <sup>46</sup>J. T. Holgate, M. Coppins, and J. E. Allen, *Appl. Phys. Lett.* **112**, 024101 (2018).
- <sup>47</sup>P. Rumbach, J. P. Clarke, and D. B. Go, *Phys. Rev. E* **95**, 053203 (2017).
- <sup>48</sup>P. Bruggeman, J. Walsh, D. Schram, C. Leys, and M. Kong, *Plasma Sources Sci. Technol.* **18**, 045023 (2009).
- <sup>49</sup>R. Morrow, D. R. McKenzie, and M. M. M. Bilek, *J. Phys. D: Appl. Phys.* **39**, 937 (2006).
- <sup>50</sup>T. Shirafuji, A. Nakamura, and F. Tochikubo, *Jpn. J. Appl. Phys.* **53**, 03DG04 (2014).
- <sup>51</sup>S. Dewan, V. Carnevale, A. Bankura, A. Eftekhari-Bafrooei, G. Fiorin, M. L. Klein, and E. Borguet, *Langmuir* **30**, 8056–8065 (2014).
- <sup>52</sup>A. Groß and S. Sakong, *Curr. Opin. Electrochem.* **14**, 1–6 (2019).
- <sup>53</sup>S. A. Norberg, E. Johnsen, and M. J. Kushner, *J. Phys. D: Appl. Phys.* **49**, 185201 (2016).
- <sup>54</sup>G. R. Medders and F. Paesani, *J. Am. Chem. Soc.* **138**, 3912–3919 (2016).
- <sup>55</sup>T. Kondo, M. Tsumaki, W. A. Diño, and T. Ito, *J. Phys. D: Appl. Phys.* **50**, 244002 (2017).
- <sup>56</sup>S. B. King, D. Wegkamp, C. Richter, M. Wolf, and J. Stähler, *J. Phys. Chem. C* **121**, 7379–7386 (2017).
- <sup>57</sup>J. M. Herbert and M. P. Coons, *Annu. Rev. Phys. Chem.* **68**, 447–472 (2017).
- <sup>58</sup>D. M. Sagar, C. D. Bain, and J. R. R. Verlet, *J. Am. Chem. Soc.* **132**, 6917–6919 (2010).
- <sup>59</sup>T. M. Chang and L. X. Dang, *Chem. Rev.* **106**, 1305–1322 (2006).
- <sup>60</sup>P. Jungwirth and B. Winter, *Annu. Rev. Phys. Chem.* **59**, 343–366 (2008).
- <sup>61</sup>K. D. Collins and M. W. Washabaugh, *Q. Rev. Biophys.* **18**, 323–422 (1985).
- <sup>62</sup>K. Tachibana and K. Yasuoka, *J. Phys. D: Appl. Phys.* **53**, 125203 (2020).
- <sup>63</sup>P. Jungwirth and D. J. Tobias, *J. Phys. Chem. B* **105**, 10468–10472 (2001).
- <sup>64</sup>J. R. Toth, R. Hawtof, D. Matthiesen, J. N. Renner, and R. M. Sankaran, *J. Electrochem. Soc.* **167**, 116504 (2020).
- <sup>65</sup>T. Smolinka, See <https://www.h2-international.com/2017/06/06/h2-production-by-water-electrolysis-technology-trends/> for “H2-international” (2017).
- <sup>66</sup>G. Oinuma, G. Nayak, Y. Du, and P. J. Bruggeman, *Plasma Sources Sci. Technol.* **29**, 095002 (2020).
- <sup>67</sup>A. A. Fridman, *Plasma Chemistry* (Cambridge University Press, 2014).
- <sup>68</sup>B. R. Locke and K. Y. Shih, *Plasma Sources Sci. Technol.* **20**, 034006 (2011).
- <sup>69</sup>S. Mohades, A. M. Lietz, and M. J. Kushner, *J. Phys. D: Appl. Phys.* **53**, 435206 (2020).
- <sup>70</sup>P. Lukes, E. Dolezalova, I. Sisrova, and M. Clupek, *Plasma Sources Sci. Technol.* **23**, 015019 (2014).
- <sup>71</sup>G. Nayak, H. A. Aboubakr, S. M. Goyal, and P. J. Bruggeman, *Plasma Processes Polym.* **15**, 1700119 (2018).
- <sup>72</sup>S. Banerjee, E. Gnanamani, X. Yan, and R. N. Zare, *Analyst* **142**, 1399–1402 (2017).
- <sup>73</sup>W. V. Gaens and A. Bogaerts, *J. Phys. D: Appl. Phys.* **46**, 275201 (2013).
- <sup>74</sup>D. X. Liu, P. Bruggeman, F. Iza, M. Z. Rong, and M. G. Kong, *Plasma Sources Sci. Technol.* **19**, 025018 (2010).
- <sup>75</sup>J. Tennyson, S. Rahimi, C. Hill, L. Tse, A. Vibhakar, D. Akello-Egwel, D. B. Brown, A. Dzarasova, J. R. Hamilton, D. Jaksch, S. Mohr, K. Wren-Little, J. Bruckmeier, A. Agarwal, K. Bartschat, A. Bogaerts, J. P. Booth, M. J. Goeckner, K. Hassouni, Y. Itikawa, B. J. Braams, E. Krishnakumar, A. Laricchiuta, N. J. Mason, S. Pandey, Z. L. Petrovic, Y. K. Pu, A. Ranjan, S. Rauf, J. Schulze, M. M. Turner, P. Ventzek, J. C. Whitehead, and J. S. Yoon, *Plasma Sources Sci. Technol.* **26**, 055014 (2017).
- <sup>76</sup>L. R. Grabowski, E. M. van Veldhuizen, A. J. M. Pemen, and W. R. Rutgers, *Plasma Chem. Plasma Process.* **26**, 3–17 (2006).
- <sup>77</sup>B. R. Locke, M. Sato, P. Sunka, M. R. Hoffmann, and J. S. Chang, *Ind. Eng. Chem. Res.* **45**, 882–905 (2006).
- <sup>78</sup>P. Lukes, A. T. Appleton, and B. R. Locke, *IEEE Trans. Ind. Appl.* **40**, 60–67 (2004).
- <sup>79</sup>Y. Zheng, L. Wang, and P. Bruggeman, *J. Vac. Sci. Technol. A* **38**, 063005 (2020).
- <sup>80</sup>H. A. Aboubakr, U. Gangal, M. M. Youssef, S. M. Goyal, and P. J. Bruggeman, *J. Phys. D: Appl. Phys.* **49**, 204001 (2016).
- <sup>81</sup>V. S. S. K. Kondeti, C. Q. Phan, K. Wende, H. Jablonowski, U. Gangal, J. L. Granick, R. C. Hunter, and P. J. Bruggeman, *Free Radic. Biol. Med.* **124**, 275–287 (2018).
- <sup>82</sup>K. Wende, P. Williams, J. Dalluge, W. Van Gaens, H. Aboubakr, J. Bischof, T. von Woedtke, S. M. Goyal, K. D. Weltmann, A. Bogaerts, K. Masur, and P. J. Bruggeman, *Biointerphases* **10**, 029518 (2015).
- <sup>83</sup>J. Benedikt, M. M. Hefny, A. Shaw, B. R. Buckley, F. Iza, S. Schäfermann, and J. E. Bandow, *Phys. Chem. Chem. Phys.* **20**, 12037–12042 (2018).
- <sup>84</sup>Y. Gorbanev, D. O'Connell, and V. Chechik, *Chem. Eur. J.* **22**, 3496–3505 (2016).
- <sup>85</sup>R. A. Marcus, *J. Chem. Phys.* **43**, 3477 (1965).
- <sup>86</sup>K. R. Siefertmann, Y. Liu, E. Lugovoy, O. Link, M. Faubel, U. Buck, B. Winter, and B. Abel, *Nat. Chem.* **2**, 274–279 (2010).
- <sup>87</sup>K. Yokoyama, C. Silva, D. H. Son, P. K. Walhout, and P. F. Barbara, *J. Phys. Chem. A* **102**, 6957–6966 (1998).
- <sup>88</sup>C. Richmonds, M. Witzke, B. Bartling, S. W. Lee, J. Wainright, C. C. Liu, and R. M. Sankaran, *J. Am. Chem. Soc.* **133**, 17582–17585 (2011).
- <sup>89</sup>M. Witzke, P. Rumbach, D. B. Go, and R. M. Sankaran, *J. Phys. D: Appl. Phys.* **45**, 442001 (2012).
- <sup>90</sup>T. Oldham, M. Chen, S. Sharkey, K. M. Parker, and E. Thimsen, *J. Phys. D: Appl. Phys.* **53**, 165202 (2020).
- <sup>91</sup>V. S. S. K. Kondeti, U. Gangal, S. Yatom, and P. J. Bruggeman, *J. Vac. Sci. Technol. A* **35**, 061302 (2017).
- <sup>92</sup>J. J. Wu, V. S. S. K. Kondeti, P. J. Bruggeman, and U. R. Kortshagen, *J. Phys. D: Appl. Phys.* **49**, 08LT02 (2016).
- <sup>93</sup>A. R. Singh, B. A. Rohr, J. A. Schwalbe, M. Cargnello, K. Chan, T. F. Jaramillo, I. Chorkendorff, and J. K. Nørskov, *ACS Catal.* **7**, 706–709 (2017).
- <sup>94</sup>Y. Gorbanev, E. Vervloessem, A. Nikiforov, and A. Bogaerts, *ACS Sustainable Chem. Eng.* **8**, 2996–3004 (2020).
- <sup>95</sup>H. E. Delgado, R. C. Radosky, D. C. Martin, D. M. Bartels, P. Rumbach, and D. B. Go, *J. Electrochem. Soc.* **166**, E181 (2019).

- <sup>96</sup>R. G. Compton and C. E. Banks, *Understanding Voltammetry* (Imperial College Press, London, 2011).
- <sup>97</sup>K. Tachibana, Y. Takekata, Y. Mizumoto, H. Motomura, and M. Jinno, *Plasma Sources Sci. Technol.* **20**, 034005 (2011).
- <sup>98</sup>O. Ogunyinka, A. Wright, G. Bolognesi, F. Iza, and H. C. H. Bandulasena, *Microfluid. Nanofluid.* **24**, 13 (2020).
- <sup>99</sup>R. Burlica and B. R. Locke, *IEEE Trans. Ind. Appl.* **44**, 482–489 (2008).
- <sup>100</sup>N. Takeuchi, M. Ando, and K. Yasuoka, *Jpn. J. Appl. Phys.* **54**, 116201 (2015).
- <sup>101</sup>S. Hamaguchi, K. Ikuse, and T. Kanazawa, *JPS Conf. Proc.* **1**, 015055 (2014).
- <sup>102</sup>H. Taghvaei, V. S. S. K. Kondeti, and P. J. Bruggeman, *Plasma Chem. Plasma Process.* **39**, 729–749 (2019).
- <sup>103</sup>P. Rumbach, D. M. Bartels, and D. B. Go, *Plasma Sources Sci. Technol.* **27**, 115013 (2018).
- <sup>104</sup>M. Shiraiwa, C. Pftrang, T. Koop, and U. Pöschl, *Atmos. Chem. Phys.* **12**, 2777–2794 (2012).
- <sup>105</sup>D. R. Grymonpré, A. K. Sharma, W. C. Finney, and B. R. Locke, *Chem. Eng. J.* **82**, 189–207 (2001).
- <sup>106</sup>S. Medodovic and B. R. Locke, *J. Phys. D: Appl. Phys.* **42**, 049801 (2009).
- <sup>107</sup>N. Takeuchi, Y. Ishii, and K. Yasuoka, *Plasma Sources Sci. Technol.* **21**, 015006 (2012).
- <sup>108</sup>N. Y. Babaeva and M. J. Kushner, *J. Phys. D: Appl. Phys.* **42**, 132003 (2009).
- <sup>109</sup>B. D. Storey and A. J. Szeri, *Proc. R. Soc. Lond. A.* **456**, 1685–1709 (2000).
- <sup>110</sup>D. X. Liu, Z. C. Liu, C. Chen, A. J. Yang, D. Li, M. Z. Rong, H. L. Chen, and M. G. Kong, *Sci. Rep.* **6**, 23737 (2016).
- <sup>111</sup>S. A. Norberg, W. Tian, E. Johnsen, and M. J. Kushner, *J. Phys. D: Appl. Phys.* **47**, 475203 (2014).
- <sup>112</sup>A. Lindsay, C. Anderson, E. Slikboer, S. Shannon, and D. Graves, *J. Phys. D: Appl. Phys.* **48**, 424007 (2015).
- <sup>113</sup>W. Tian, A. M. Lietz, and M. J. Kushner, *Plasma Sources Sci. Technol.* **25**, 055020 (2016).
- <sup>114</sup>C. Chen, D. Liu, A. Yang, H. L. Chen, and M. G. Kong, *Plasma Chem. Plasma Process.* **38**, 89–105 (2018).
- <sup>115</sup>G. V. Buxton, C. L. Greenstock, W. P. Helman, and A. B. Ross, *J. Phys. Chem. Ref. Data* **17**, 513–886 (1988).
- <sup>116</sup>K. P. Madden and S. P. Mezyk, *J. Phys. Chem. Ref. Data* **40**, 023103 (2011).
- <sup>117</sup>R. E. Huie, See <http://kinetics.nist.gov/solution> for “NDRL/NIST Solution Kinetics Database on the WEB,” National Institute of Standards and Technology (2003).
- <sup>118</sup>R. D. Hudson, *Rev. Geophys.* **9**, 305–406 (1971).
- <sup>119</sup>N. Getoff and G. O. Schenck, *Photochem. Photobiol.* **8**, 167–178 (1968).
- <sup>120</sup>C. E. Kolb, R. A. Cox, J. P. D. Abbatt, M. Ammann, E. J. Davis, D. J. Donaldson, B. C. Garrett, C. George, P. T. Griffiths, D. R. Hanson, M. Kulmala, G. McFiggans, U. Pöschl, I. Riipinen, M. J. Rossi, Y. Rudich, P. E. Wagner, P. M. Winkler, D. R. Worsnop, and C. D. O’Dowd, *Atmos. Chem. Phys.* **10**, 10561–10605 (2010).
- <sup>121</sup>T. Berkemeier, A. J. Huisman, M. Ammann, M. Shiraiwa, T. Koop, and U. Pöschl, *Atmos. Chem. Phys.* **13**, 6663–6686 (2013).
- <sup>122</sup>P. Davidovits, C. E. Kolb, L. R. Williams, J. T. Jayne, and D. R. Worsnop, *Chem. Rev.* **106**, 1323–1354 (2006).
- <sup>123</sup>V. S. S. K. Kondeti, Y. Zheng, P. Luan, G. S. Oehrlein, and P. J. Bruggeman, *J. Vac. Sci. Technol. A* **38**, 033012 (2020).
- <sup>124</sup>A. D. Lindsay, D. B. Graves, and S. C. Shannon, *J. Phys. D: Appl. Phys.* **49**, 235204 (2016).
- <sup>125</sup>M. J. Grapperhaus and M. J. Kushner, *J. Appl. Phys.* **81**, 569 (1997).
- <sup>126</sup>S. Schnur and A. Groß, *New J. Phys.* **11**, 125003 (2009).
- <sup>127</sup>N. A. Garland, I. Simonović, G. J. Boyle, D. G. Cocks, S. Duijko, and R. D. White, *Plasma Sources Sci. Technol.* **27**, 105004 (2018).
- <sup>128</sup>H. Bluhm, *Pulsed Power Systems: Principles and Applications* (Springer-Verlag, 2006).
- <sup>129</sup>J. Benedikt, A. Hecimovic, D. Ellerweg, and A. von Keudell, *J. Phys. D: Appl. Phys.* **45**, 403001 (2012).
- <sup>130</sup>A. F. H. van Gessel, E. A. D. Carbone, P. J. Bruggeman, and J. J. A. M. van der Mullen, *Plasma Sources Sci. Technol.* **21**, 015003 (2012).
- <sup>131</sup>T. Verreycken, R. M. van der Horst, N. Sadeghi, and P. J. Bruggeman, *J. Phys. D: Appl. Phys.* **46**, 464004 (2013).
- <sup>132</sup>S. Yatomi, Y. Luo, Q. Xiong, and P. J. Bruggeman, *J. Phys. D: Appl. Phys.* **50**, 415204 (2017).
- <sup>133</sup>P. Bruggeman, G. Cunge, and N. Sadeghi, *Plasma Sources Sci. Technol.* **21**, 035019 (2012).
- <sup>134</sup>R. E. Ardrey, *Liquid Chromatography—Mass Spectrometry: An Introduction* (John Wiley & Sons, Ltd, 2003).
- <sup>135</sup>R. F. P. Nogueira, M. C. Oliveira, and W. C. Paterlini, *Talanta* **66**, 86–91 (2005).
- <sup>136</sup>H. Tresp, M. U. Hammer, J. Winter, K. D. Weltmann, and S. Reuter, *J. Phys. D: Appl. Phys.* **46**, 435401 (2013).
- <sup>137</sup>B. He, Y. Ma, X. Gong, Z. Long, J. Li, Q. Xiong, H. Liu, Q. Chen, X. Zhang, S. Yang, and Q. H. Liu, *J. Phys. D: Appl. Phys.* **50**, 445207 (2017).
- <sup>138</sup>D. M. Bartels, K. Takahashi, J. A. Cline, T. W. Marin, and C. D. Jonah, *J. Phys. Chem. A* **109**, 1299–1307 (2005).
- <sup>139</sup>N. Hodnik, G. Dehm, and K. J. J. Mayrhofer, *Acc. Chem. Res.* **49**, 2015–2022 (2016).
- <sup>140</sup>R. C. Prince, R. R. Frontiera, and E. O. Potma, *Chem. Rev.* **117**, 5070–5094 (2017).